

# **STRUCTURAL RELIABILITY ANALYSIS WITH IMPRECISE UNCERTAINTIES**

Thesis

Submitted in partial fulfilment of the requirements for the degree of

**DOCTOR OF PHILOSOPHY**

by

**SPOORTHI S K**

**(CV15F11)**



**DEPARTMENT OF CIVIL ENGINEERING  
NATIONAL INSTITUTE OF TECHNOLOGY KARNATAKA  
SURATHKAL, MANGALURU – 575 025**

**FEBRUARY, 2021**



# **STRUCTURAL RELIABILITY ANALYSIS WITH IMPRECISE UNCERTAINTIES**

Thesis

Submitted in partial fulfilment of the requirements for the degree of

**DOCTOR OF PHILOSOPHY**

by

**SPOORTHY S K  
(CV15F11)**

Under the Guidance of

**Dr. A. S. BALU**



**DEPARTMENT OF CIVIL ENGINEERING  
NATIONAL INSTITUTE OF TECHNOLOGY KARNATAKA  
SURATHKAL, MANGALURU – 575 025**

**FEBRUARY, 2021**



## DECLARATION

I hereby *declare* that the Research Thesis entitled “**Structural Reliability Analysis with Imprecise Uncertainties**” which is being submitted to the **National Institute of Technology Karnataka, Surathkal** in partial fulfilment of the requirements for the award of the Degree of **Doctor of Philosophy in Civil Engineering**, is a *bona fide* report of the research work carried out by me. The material contained in this Research Thesis has not been submitted to any University or Institution for the award of any degree.

(SPOORTHI S K)

Register No.155099CV15F11

Department of Civil Engineering

Place: NITK, Surathkal

Date: 01-02-2021



## **CERTIFICATE**

This is to *certify* that the Research Thesis entitled “**Structural Reliability Analysis with Imprecise Uncertainties**” submitted by **Ms. SPOORTHI S K** (Register Number: **155099CV15F11**) as the record of the research work carried out by her, is accepted as the Research Thesis submission in partial fulfilment of the requirements for the award of degree of Doctor of Philosophy.

Dr. A. S. Balu

Research Guide

(Signature with date and seal)

Prof. K. Swaminathan

Chairman - DRPC

(Signature with date and seal)





## **ACKNOWLEDGEMENT**

I would like to express my sincere gratitude to my thesis supervisor Dr. A. S. Balu, Department of Civil Engineering, National Institute of Technology Karnataka, Surathkal, for the continuous support, for his patience, motivation, and immense knowledge. His selfless and systematic guidance and encouragement has helped me in all the time of research and writing of this thesis.

I would like to thank the members of RPAC, Prof. K. Swaminathan, Department of Civil Engineering, Dr. Satyanarayana Engu, and Dr. V. Murugan, Department of Mathematical and Computational Sciences, for their insightful comments and suggestions, during the progress of the research work which has helped me to shape my thesis.

I am thankful to Prof. Varghese George, former Head of the Civil Engineering Department and Prof. K. Swaminathan, Head of the Civil Engineering Department for their support during my Ph.D period. I also wish to thank all faculty members and non-teaching staff of Civil Engineering Department for their help provided during the research work.

I would like to thank my research team members B. O. Naveen, B. Kesava Rao and M. Nagesh, for their suggestions and for the valuable and enlightening discussions. I extend my thanks to my fellow research scholars Anila Cyril, S. Anaswara, M. P. Vibhoosha, Pooja Raj and Nithya R. Govind for their morale support. I thank postgraduate students especially Hitha Zacharias and Akshay Prasad, with whom I had an opportunity to share knowledge. I also thank all the research scholars of Civil Engineering Department for providing healthy research environment.

My acknowledgement would be incomplete without thanking my biggest source of my strength, my parents Mr. ShankarRao Kulkarni and Mrs. Suneeta Kulkarni. This dissertation would not have been possible without their warm love, continued patience, and endless support.

**SPOORTHI S K**



## ABSTRACT

Analysis and design involves consideration of many factors which are inherently uncertain. Reliability analysis requires information about the uncertainties in the system, and structural reliability is the probability of a structure performing its purpose adequately for the period of time intended under the operating conditions encountered. Many approaches developed for dealing with the uncertainties demand a mathematical representation of uncertainties on the basis of available information. Probability theory is the most customary technique to describe the uncertainties as random variables characterised by the probability density functions (PDF). However, if the data is inaccurate, ambiguous and incomplete, it is inept to form the PDF, and hence the conventional probabilistic approach becomes inadequate. Therefore, the imprecise parameters should be treated appropriately for improving the reliability of the system.

If the information about the uncertainty is insufficient and non-stochastic in nature, the approaches based on interval analysis or fuzzy set theory can be adopted in uncertainty quantification. Hybrid approaches are also available to handle the situations where both the nature of uncertainties namely aleatory and epistemic are uniquely present in the system. In reality, when the aleatory uncertainty is characterised with imprecise parameters, none of the above approaches yields a reliable and optimum design. In such situations, the concepts of probability-box (p-box) can be adopted for characterising the uncertainties.

Uncertainty analysis of multi-dimensional and highly nonlinear structures using simulation-based methods is cumbersome, and the hybridity demands the exploration of entire domain of bounds on imprecision. Response surface methods facilitate surrogate models to reduce the effort involved during the simulation. High dimensional model representation (HDMR) is a computationally efficient technique developed for the parameter interaction in physical problems.

Therefore, in the present work, HDMR based uncertainty analysis is developed for estimating the structural reliability in the presence of various imprecise uncertainties. The methodology involves characterising the imprecise uncertainties as p-box variables, developing limit state functions using HDMR techniques, and estimating the reliability by interval Monte-Carlo simulations. Furthermore, as the

prediction of structural behaviour might diverge due to the presence of various uncertainties, an attempt has been made by studying the systems with hybrid uncertainties from four different sources. The results of the numerical examples are compared with the traditional approaches to demonstrate the efficiency of the methodology.

**Keywords:** High dimensional model representation; Imprecise uncertainty; Interval Monte Carlo simulation; Probability-box; Structural reliability.

# CONTENTS

	<b>Page No.</b>
<b>LIST OF FIGURES</b>	<b>v</b>
<b>LIST OF TABLES</b>	<b>vii</b>
<b>ABBREVIATIONS</b>	<b>ix</b>
<b>SYMBOLS</b>	<b>xi</b>
<b>1 INTRODUCTION</b>	<b>1</b>
1.1 STRUCTURAL SAFETY	1
1.2 STRUCTURAL RELIABILITY	2
1.3 METHODS FOR STRUCTURAL RELIABILITY ANALYSIS	3
1.3.1 Monte Carlo Simulation	4
1.3.2 First Order Reliability Method	4
1.3.3 Second Order Reliability Method	5
1.4 UNCERTAINTY	5
1.4.1 Classification of Uncertainties	6
1.4.2 Imprecise Uncertainties	7
1.5 RESPONSE SURFACE METHODOLOGY	8
1.5.1 Meta-modelling Methods	8
1.5.2 High Dimensional Model Representation	9
1.6 ORGANISATION OF THESIS	12
<b>2 LITERATURE REVIEW</b>	<b>13</b>
2.1 GENERAL	13
2.2 STRUCTURAL RELIABILITY	14
2.3 IMPRECISE UNCERTAINTY	15
2.4 SURROGATE MODELLING	18
2.5 SUMMARY OF LITERATURE REVIEW	21
2.6 RESEARCH OBJECTIVES	22
2.7 SCOPE OF PRESENT RESEARCH	23

<b>3</b>	<b>HDMR BASED UNCERTAINTY ANALYSIS</b>	<b>23</b>
3.1	UNCERTAINTY ANALYSIS	23
3.1.1	Failure Probability and Reliability Index	25
3.1.2	Probability-box	29
3.1.3	Construction of p-box	30
3.2	HIGH DIMENSIONAL MODEL REPRESENTATION	32
3.3	NUMERICAL EXAMPLES	36
3.3.1	Explicit Cubic Function	37
3.3.2	Nonlinear Response Function	38
3.3.3	Creep-Fatigue Interaction	39
3.3.4	Fracture of Turbine Disk	41
3.3.5	Portal Frame Structure	43
3.3.6	Plane Truss Structure	46
<b>4</b>	<b>HYBRID STRUCTURAL RELIABILITY</b>	<b>49</b>
4.1	HYBRID UNCERTAINTIES	49
4.2	RELIABILITY ANALYSIS WITH MIXED UNCERTAINTIES	50
4.2.1	Hollow Cantilever Tube Structure	52
4.2.2	Ten-Storey Irregular RCC Structure	55
4.2.3	Nuclear Containment Structure	59
4.3	RELIABILITY ANALYSIS WITH HYBRID UNCERTAINTIES	65
4.3.1	Cantilever Beam Structure	65
4.3.2	Plane Truss Structure	66
<b>5</b>	<b>SUMMARY AND CONCLUSION</b>	<b>69</b>
5.1	RESULTS AND DISCUSSION	69
5.2	CONCLUSIONS	71
5.3	SCOPE FOR FUTURE WORK	72
	<b>REFERENCES</b>	<b>73</b>
	<b>PUBLICATIONS</b>	<b>83</b>

## LIST OF FIGURES

<b>Figure No.</b>	<b>Description</b>	<b>Page No.</b>
Figure 1.1	Concept of limit state function	2
Figure 1.2	Probability density function of $g(\mathbf{X})$	3
Figure 1.3	Illustration of difference between variability and uncertainty	6
Figure 1.4	Comparison of certainty and uncertainty	7
Figure 1.5	Meta-modelling methods and corresponding sampling techniques	11
Figure 3.1	Sources of uncertainties	24
Figure 3.2	Failure probability of deterministic strength of structure ( $Y$ )	26
Figure 3.3	Failure probability of strength ( $Y$ ) and load effect ( $W$ )	26
Figure 3.4	Concept of reliability	27
Figure 3.5	P-box with a mean [2, 3] and standard deviation 0.5	32
Figure 3.6	Sampling scheme for first-order HDMR: (a) for a function with one variable and (b) for a function with two variables	35
Figure 3.7	Flowchart for the first-order HDMR based function	36
Figure 3.8	CDF of explicit function in Eq. (3.33)	37
Figure 3.9	CDF of explicit nonlinear function in Eq. (3.34)	38
Figure 3.10	CDF of limit state function for creep-fatigue interaction	40
Figure 3.11	Model of turbine disk	41
Figure 3.12	CDF of limit state function for turbine disk	43
Figure 3.13	Portal frame structure	44
Figure 3.14	CDF of limit state function for portal frame structure	45
Figure 3.15	Plane truss structure	46
Figure 3.16	CDF of limit state function for plane truss structure	47
Figure 4.1	Flowchart for first-order HDMR failure probability for hybrid uncertainties	51
Figure 4.2	Hollow cantilever tube structure	52
Figure 4.3	FE model of hollow cantilever tube structure	53
Figure 4.4	Deformed shape of hollow cantilever tube structure; (a) Mises stress; (b) Displacement	54

Figure 4.5	CDF of limit state function for hollow cantilever tube structure	54
Figure 4.6	Plan and elevation details	56
Figure 4.7	Hinge formation at reference $c$ for (a) Irregular structure at 10th step; (b) Regular structure at 12th step	57
Figure 4.8	CDF of limit state function for irregular structure	58
Figure 4.9	CDF of limit state function for regular structure	58
Figure 4.10	Cross section details of axisymmetric model	60
Figure 4.11	Section view of nuclear containment model	61
Figure 4.12	Developed view of the hoop & vertical tendons	61
Figure 4.13	(a) Dome tendons; and (b) Hoop and vertical tendons	62
Figure 4.14	(a) FE meshing of the model; (b) Deformed at self-weight and pre-stressed load; (c) Deformed at design pressure load; (d) Deformed at ULC on dome; and (e) Deformed at ULC on opening	64
Figure 4.15	CDF of limit state function for nuclear containment structure	65
Figure 4.16	Cantilever beam structure	66
Figure 4.17	Failure probability curves of cantilever beam structure	67
Figure 4.18	Failure probability curves of plane truss structure with hybrid uncertainties	67



## LIST OF TABLES

<b>Table No.</b>	<b>Description</b>	<b>Page No.</b>
Table 1.1	Meta-modelling techniques	10
Table 3.1	Description of sources of uncertainties	24
Table 3.2	Response bounds of explicit function in Eq. (3.33)	38
Table 3.3	Response bounds of explicit nonlinear function in Eq. (3.34)	39
Table 3.4	Input parameters for creep-fatigue interaction	39
Table 3.5	Bounds of creep-fatigue interaction	41
Table 3.6	Failure probability and reliability index of creep-fatigue interaction	41
Table 3.7	Input parameters for turbine disk	42
Table 3.8	Fracture strength of turbine disk	42
Table 3.9	Failure probability and reliability index of turbine disk	43
Table 3.10	Input parameters for portal frame structure	44
Table 3.11	Horizontal displacement (in mm) of the portal frame structure	45
Table 3.12	Failure probability and reliability index of portal frame structure	45
Table 3.13	Input parameters for plane truss structure	46
Table 3.14	Vertical deflection of plane truss structure	47
Table 3.15	Failure probability and reliability index of plane truss structure	47
Table 4.1	Input mixed uncertainties for hollow cantilever tube structure	53
Table 4.2	Von-Mises stress of hollow cantilever tube structure	54
Table 4.3	Failure probability and reliability index of hollow cantilever tube structure	55
Table 4.4	Input parameters for irregular and regular structures	56
Table 4.5	Horizontal displacement of irregular and regular structures	57
Table 4.6	Failure probability and reliability index of irregular and regular structures	59
Table 4.7	Material properties based on test data	63
Table 4.8	Input mixed uncertainties for nuclear containment structure	64

Table 4.9	Failure probability and reliability index of nuclear containment structure	65
Table 4.10	Input hybrid uncertainties for cantilever beam structure	66
Table 4.11	Input hybrid uncertainties for plane truss structure	68

## ABBREVIATIONS

AERB	Atomic Energy Regulatory Board
AK-MCS	Adaptive Kriging Monte Carlo Simulation
ALK	Active Learning Kriging artificial neural network
ANN	Artificial Neural Network
ANOVA	Analysis of Variance
BLUP	Best Linear Unbiased Predictor
CCD	Central Composite Design
CDF	Cumulative Distribution Function
CDP	Concrete Damaged Plasticity
CP	Collapse Prevention
EGO	Efficient Global Optimization
FE	Finite Element
FFNI	Full Factorial Numerical Integration
FORM	First Order Reliability Method
GA	Genetic Algorithm
GMDH	Group Method of Data Handling
GUI	Graphical User Interface
HDMR	High Dimensional Model Representation
IFEM	Interval Finite Element Method
I-HDMR	Indexing HDMR
IMCS	Interval Monte Carlo Simulation
IO	Immediate Occupancy
LB	Lower Bound
LH	Latin Hypercube
LS	Life Safety
KLE	Karhunen-Loeve Expansions
MARS	Multivariate Adaptive Regression Splines
MCS	Monte Carlo Simulation
MLS	Moving Least Square
MPA	Multi-Point Approximation

MPP	Most Probable Point
OIMCS	Optimization based Interval Monte Carlo simulation
p-box	Probability-box
PCA	Principle Component Analysis
PCE	Polynomial Chaos Expansion
PDF	Probability Density Function
PMA	Performance Measurement Approach
PNN	Polynomial Neural Network
PR	Polynomial Regression
$\mathbb{R}$	Real Number
R	Reliability
RBF	Radial Basis Functions
RCC	Reinforced Cement Concrete
RIA	Reliability Index Approach
RS	Random Sampling
RSM	Response Surface Method
SORM	Second Order Reliability Method
SVM	Support Vector Machine
SVR	Support Vector Regression
UB	Upper Bound
ULC	Ultimate Load Capacity

## SYMBOLS

$\beta$	Reliability index
$\mu_g$	Mean of $g(\mathbf{X})$
$\sigma_g$	Standard deviation of $g(\mathbf{X})$
$\sigma_{\max}$	Maximum stress
$\sigma_{pt}$	Pre-stress load
$\sigma_x$	Normal stress
$\tau_{zx}$	Torsional stress
$\phi_j(x_i)$	Lagrange's interpolation term
$\Phi$	Standard normal cumulative distribution function
$\Delta_h$	Horizontal displacement
$\Delta_{\lim}$	Limit of displacement
$\delta_{\lim}$	Limit of deflection
$\delta_{\max}$	Maximum deflection
$\delta_v$	Vertical deflection
$A$	area of cross section
$a$	Initial crack length
$a_0$	Radius of initial crack
$A_t$	Cross-sectional area of tendons
$b_b$	Width of beam
$b_c$	Width of column
$c$	Reference point
$c$	Crack propagation
$d$	Diameter of hollow cantilever tube
$d_b$	Depth of beam
$D_c$	Creep damage

$d_c$	Depth of column
$D_f$	Fatigue damage
$E$	Modulus of elasticity
$E_c$	Modulus of elasticity of concrete
$F$	Failure domain
$F_c$	Correction factor
$F(x)$	Cumulative distribution function of $X$
$f_{ck}$	Cube strength
$f_g(g)$	Probability density function of $g(\mathbf{X})$
$f_{\mathbf{X}}(\mathbf{x})$	Joint Probability density function
$f_y$	Yield strength
$g_0$	Response of the system at mean input parameters
$g_i(x_i)$	First order term
$g(x_i, c_i)$	First order component function
$g_{i_1 i_2}(x_{i_1}, x_{i_2})$	Second order term
$g(\mathbf{X})$	Limit state function
$\tilde{g}(\mathbf{X})$	HDMR approximation function
$g(\mathbf{X}) = 0$	Limit state surface
$g(\mathbf{X}) > 0$	Safe domain
$g(\mathbf{X}) \leq 0$	Failure domain
$I$	Moment of inertia
$I[\cdot]$	Indicator function
$K_{IC}$	Critical fracture toughness
$K_{\max}$	Stress intensity factor
$L$	Length of member
$LL$	Live load
$M$	Bending moment
$m$	Crack propagation index

$N$	Number of input variables
$n$	Number of sample points
$N_c$	Life of creep
$n_c$	Number of loading cycles for creep
$N_F$	Number of failure events
$N_f$	Life of fatigue
$n_f$	Number of loading cycles for fatigue
$N_s$	Number of function evaluation
$P$	Load on the structure
$P_d$	Load design pressure load
$P_f$	Failure probability
$\underline{P}(E)$	Lower probability of an event
$\bar{P}(E)$	Upper probability of an event
$s$	Order of the component function
$T$	Torsion
$t$	Thickness of hollow cantilever tube
$\mathbf{X}$	Vector of input variables
$X$	Input variable
$\mathbf{x}$	Realization vector
$x$	Realization of variable
$[\underline{x}, \bar{x}]$	Lower and upper bounds of the interval
$Y$	Resistance/strength of the structure
$W$	Action/load effect on the structure





# CHAPTER 1

## INTRODUCTION

### 1.1 STRUCTURAL SAFETY

The performance of a structure is evaluated by its safety, serviceability and economy. Safety assessment of structures is a task of much importance. Safety of a structure depends on action on the structure and its resistance to the action. The action is a function of load acting on the structure and resistance which depends on material property as well as geometry of the structure. Generally, these parameters are subjected to statistical variations and are probabilistic or random variables. Necessary attempt was made for the evaluation of safety by including statistical variation of parameters, hence research started on safety of structures, by considering the random variations of these parameters from 1960.

Design methods for structural systems are mainly categorised as permissible stress method or working stress design method, ultimate strength method and limit state method. In the first method, only the stresses occurring under maximum service loads were compared with permissible stresses. Hence, the safety is defined in terms of factor of safety, which is given by,

$$\text{Factor of safety} = \frac{\text{failure stress}}{\text{permissible stress}} \quad (1.1)$$

In ultimate stress method, safety was ensured by introducing ultimate load factor, which is the magnification factor of service loads, defined as,

$$\text{Ultimate load factor} = \frac{\text{ultimate load}}{\text{service load}} \quad (1.2)$$

There was a limitation in assessing the safety by these methods, and therefore the limit state method was introduced. In this there are two categories, ultimate limit state and serviceability limit state. These are conventional methods based on the factors affecting the safety in the design of structures. On the other hand, risk and reliability can be evaluated by, deterministic (non-probabilistic) and probabilistic methods, which consider the safety conditions. As the name says, in the deterministic method, the parameters of the structures are considered to be deterministic (not subjected to

probabilistic variations), while, the parameters are considered as random variables in the probabilistic method. However, it is a fact that, loads (live load on floors, wind load, ocean waves, earthquake, etc.), strength of materials (material properties of concrete and steel, etc.), and geometric parameters (sectional dimensions of frame elements, effective depth, diameter of the reinforcement, etc.) are subjected to statistical variations. Hence, it is important to consider the statistical variations in estimating the structural safety.

The information about input variables (loads, material property and geometric parameters) is never certain, precise or complete. Such imprecise and incomplete information about input variables are considered as uncertainties. Risk and safety of the structure is generally estimated in terms of reliability or failure probability.

## 1.2 STRUCTURAL RELIABILITY

Structural reliability is defined as the performance of a system not exceeding the threshold limit with given constraints. Structural reliability analysis aims at assessing the probability of occurrence of an extreme event related to a given structure. Reliability estimation demands evaluation of probability that a structural response oversteps a threshold limit, defined by a limit state function governed by assorted random parameters, denoted as  $g(\mathbf{X})$ . The concept of limit state function is illustrated in Fig. 1.1 and probability density functions (PDF) of  $g(\mathbf{X})$  is shown in Fig. 1.2. The notation  $g(\mathbf{X}) = 0$ ,  $g(\mathbf{X}) > 0$  and  $g(\mathbf{X}) \leq 0$  denote limit state surface, safe domain and failure domain respectively.

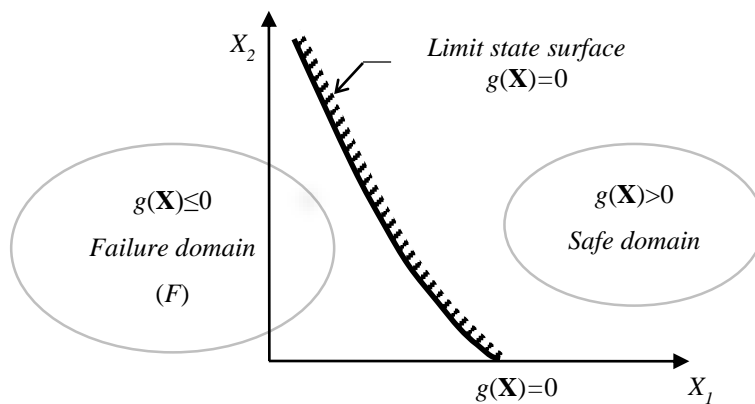


Fig. 1.1 Concept of limit state function

In the usual setting, limit state function describes the safety level of the structure for a given input vector  $\mathbf{X} \in \mathbb{R}$ . Also, the failure domain  $F$ , i.e.  $F = \{\mathbf{X} \in \mathbb{R} \mid g(\mathbf{X}) \leq 0\}$  corresponds to the set of inputs for which the limit state function  $g(\mathbf{X}) \leq 0$ . Therefore, reliability can also be measured as, probability of failure of the system with given input vector  $\mathbf{X}$ , which is  $R = 1 - P_f$ . The failure probability ( $P_f$ ) is mathematically stated as the evaluation of multi-dimensional integral as,

$$P_f = P(g(\mathbf{X}) \leq 0) = \int_{g(\mathbf{X}) \leq 0} f_{\mathbf{x}}(\mathbf{x}) dx \quad (1.3)$$

here,  $\mathbf{X} = \{X_1, X_2, \dots, X_N\}$  is  $N$ -dimensional vector of random variables of the system under observation, and  $f_{\mathbf{x}}(\mathbf{x})$  is the joint PDF of the influencing input variables. Probability theory is traditionally used for the reliability assessment wherein all the uncertain variables are random in nature.

### 1.3 METHODS FOR STRUCTURAL RELIABILITY ANALYSIS

Reliability analysis evaluates the failure probability of structural systems by determining whether the limit state function is exceeding the threshold value or not. However, reliability analysis is not limited to calculation of the failure probability. Several methods have been developed for reliability analysis in last few decades including enriched performance measure approach, complementary interaction method, sequential optimization, dimension reduction method, Bayesian reliability analysis method etc.

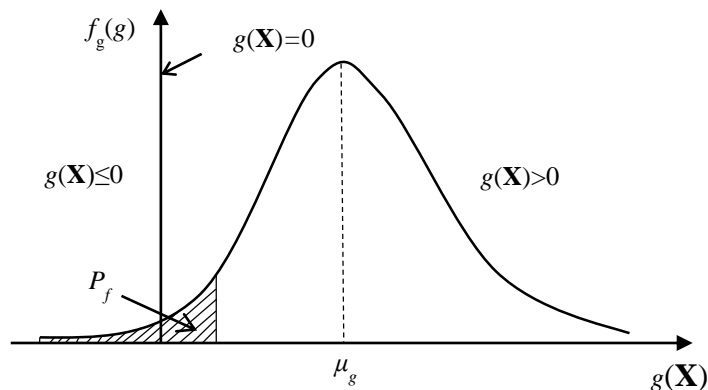


Fig. 1.2 Probability density function of  $g(\mathbf{X})$

Reliability assessment requires statistical knowledge about input parameters including probability distribution and statistical moments. In case, the input data is large and/or the knowledge about the variables are ambiguous, formulating the mathematical model of an existing system becomes tedious. In such situations, simulation techniques like Monte Carlo simulation (MCS) method is the only tool that can be used to get the relevant answers. Response surface methods were also developed for systems with large number of variables, in order to reduce the computational efficiency (Wang and Chen 2016). There are well established traditional algorithms such as first order reliability method (FORM) and second order reliability method (SORM) which have grabbed the attention for probabilistic reliability assessment.

### 1.3.1 Monte Carlo Simulation

Monte Carlo Simulation (MCS) is a sampling method which generates random samples for uncertain variables as statistical trials that make realisation based on generated samples. It approximates probability of a specific event out of a series of stochastic processes. In case of structural reliability analysis, sampling of random variables are generated according to the PDF, then a mathematical model or limit state function  $g(\mathbf{X})$  consisting the random samples is set to determine failure probability. Finally, probabilistic characteristics of the system response can be extracted through the simulation for  $N_s$  trials. Hence the failure probability is calculated as a ratio of number of failure events ( $N_f$ ) to the number of function evaluations ( $N_s$ ), given by,

$$P_f = \frac{N_f}{N_s} \quad (1.4)$$

MCS is robust and easy to operate, but impractical to generate more samples for realistic problems where each response computation may require dynamic analysis of nonlinear structural system.

### 1.3.2 First Order Reliability Method

In many engineering applications,  $g(\mathbf{X})$  is a black-box model (or simulation model), and the evaluation of  $g(\mathbf{X})$  is computationally expensive. Examples of black-box models include finite element analysis, dynamic simulation, and computational fluid dynamics. Because of the complexities, there is seldom an analytical solution to the probability integration, except for very special cases. It is also impractical using

numerical integration to find the solution due to the high dimensionality in most engineering applications. Therefore, approximation methods, such as the FORM and SORM have been developed for evaluating structural reliability.

FORM is one of the most commonly used reliability analysis methods. Basic idea of the method is to ease the computational difficulties through simplifying the integrand  $f_x(\mathbf{x})$  and approximating the function  $g(\mathbf{X})$  (Ditlevsen and Madsen, 1996; Li and Foschi, 1998). The basic concepts of FORM is, transformation of arbitrary random uncertainty vectors into independent, standard normal vectors and approximation of the boundaries of component failure domains by linear or quadratic expansions in a certain point on the failure boundary so that failure probabilities can simply be estimated from the probabilities of linear or quadratic forms in normal variables (Choi et al. 2007).

### **1.3.3 Second Order Reliability Method**

FORM usually works well when the limit-state surface has only one minimal distance point and the function is nearly linear in the neighbourhood of the design point. However, if the failure surface has large curvatures (high nonlinearity), the failure probability estimated by FORM using the reliability index may give unreasonable and inaccurate results. To resolve this problem, the second-order Taylor series (or other polynomials) is considered. The main limitation of FORM/SORM is that, the limit state functions need to be specified explicitly.

## **1.4 UNCERTAINTY**

Uncertainty is lack of certainty or imperfection about a quantity. Uncertainties influencing both structural parameters and imposed loads are important in the prediction of behaviour of the structure. Generally, parameters of the system are assumed to be deterministic, although real-world problems accommodate numerous uncertainties in design, service and ageing of the system. In order to maintain design safety, the impact of uncertainties has to be treated according to the needs of the situation. There are various connotations about uncertainties, such as variability, inaccuracy, degree of belief, likelihood of events, etc. But these representations may yield different interpretation of inaccuracy about a given quantity. Fig. 1.3 illustrates difference between variability and uncertainty.

### 1.4.1 Classification of Uncertainties

The competence and limitations of different representations have been delineated by classifying uncertainties into two categories: aleatory and epistemic. Considering these two uncertainty factors comprehensively, some theoretical literature research studies were carried out in recent years. Aleatory uncertainty is inherent and irreducible. Epistemic uncertainty is reducible that stems from lack of knowledge and data. Random variables/fields are part of aleatory uncertainties, wherein imprecise uncertainties fall into the latter category. Probability theory is the most customary technique to describe the uncertainties as random variables characterised by the PDF. In real-world scenario the uncertainty need not be equivalent to randomness, therefore classic probability approach is not an answer for incorporating such uncertainty. The difference between these theories is depicted in Fig. 1.4, which distinguishes the certainty with deterministic values of constant quantities and uncertainty by probability or interval information and other approaches.

In most of the situations, information about the uncertainty may be non-stochastic in nature. Many approaches have been developed to deal with uncertainties for studying the system responses. These approaches demand a mathematical representation of uncertainties on the basis of available information. In this context, the approaches based on interval analysis or fuzzy set theory can be adopted in uncertainty quantification.

Intervals represent range of values falling under upper and lower bounds, and do not involve any knowledge on cumulative distribution function (CDF) of values within the bounds. Interval field is the non-stochastic counterpart of the random field. Intervals are employed to represent spatial nondeterministic response of structural systems under various loading conditions (Faes and Moens 2019; Gao et al. 2018; Xiao et al. 2015).

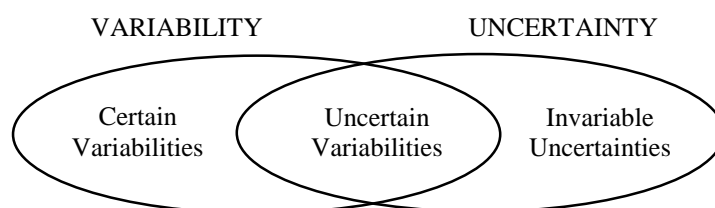


Fig. 1.3 Illustration of difference between variability and uncertainty (Moens and Vandepitte 2004)

Fuzzy set theory presents a concept for the description of instinctive knowledge and incomplete data in a non-probabilistic way. Fuzzy set introduces membership function, a degree of belongingness. Commonly adopted membership function shapes are triangular and Gaussian. Fuzzy finite element method is broadly accepted for non-deterministic parameters in FE models (Balu and Rao 2012a; Lü et al. 2016; Zhang et al. 2018).

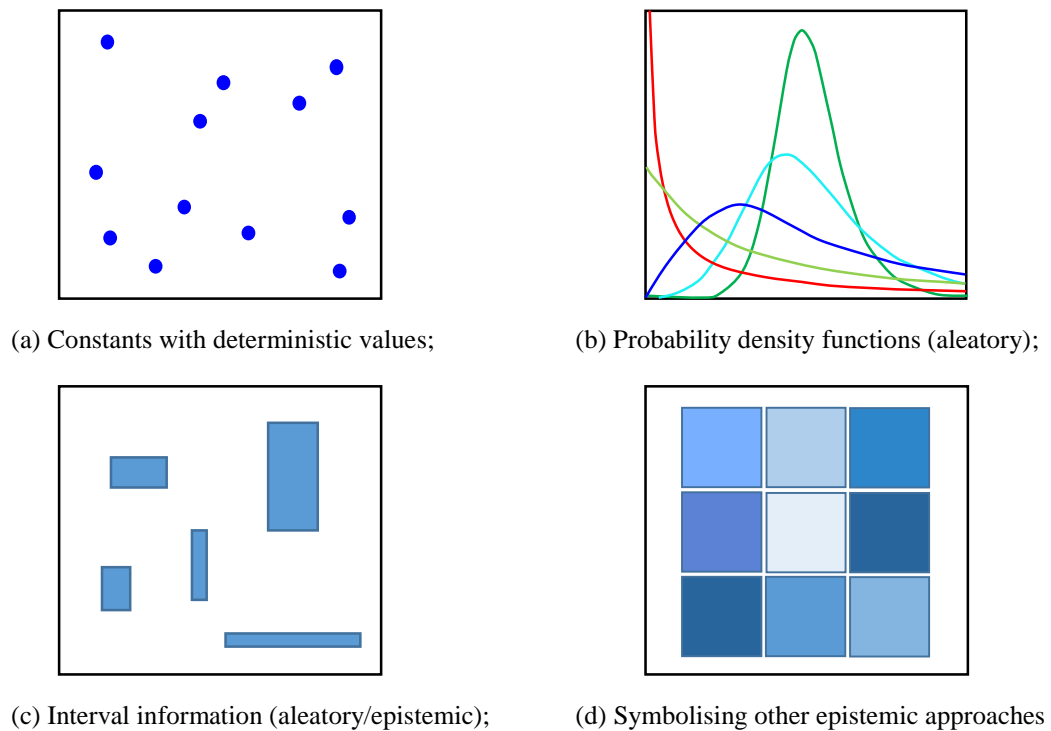


Fig. 1.4 Comparison of certainty and uncertainty (Hou et al. 2019)

### 1.4.2 Imprecise Uncertainties

The design of civil engineering constructions frequently involves a great uncertainty about loading conditions, material properties and their degradation in time, human errors in modeling, construction and successive management. Information about an uncertain quantity under consideration is termed as imprecise when it is expressed as a set of possible values (rather deterministic) that the quantity may have. Source of such uncertainties can be dependency relationship, limited experimental data, material quality issues, inconsistent measurement data, inaccuracy in the way mathematical equations are solved (numerical uncertainty), imprecision in the way model parameters are defined (parameter uncertainty), etc. For example, the uncertainty associated with

modeling a boundary condition depends on the selected representation of the boundary (structural uncertainty), and the input parameters entered to define the boundary condition (parameter uncertainty). Therefore, these sources of uncertainty must be studied to quantify their degrading effects on the predictive capabilities of a computer model (Christie et al. 2005). One way to model imprecise probabilities is to represent a probability with the interval between the lowest possible and the highest possible probability, respectively. Probability-box is another conventional framework to represent imprecisely specified distributions.

## **1.5 RESPONSE SURFACE METHODOLOGY**

Design of any structure needs excessive time for experiments and expensive simulations, which make design costly. Complex systems with multiple input variables, increase the severity of the design. Finite element (FE) model based simulation is one of the popular tools widely adopted for the analysis. The cost of performing such analyses that depends upon computational model, type of analysis, and uncertainty conditions is high and uneconomic. To minimize the number of performance function computations and to get the accurate estimation of responses, response surface methods (RSM) are available. Response surface methodology is a collection of mathematical and statistical techniques for empirical model building. The main objective of RSM is to optimize output variable, which is governed by several independent input variables, by set of experiments. These experiments are series of tests, called runs, in which, modification is made in the input variables for the study of behaviour of output response. Application of RSM aims at reducing the cost of conventional methods. RSMs facilitate meta-models to reduce the effort involved during the simulation. These techniques are based on optimization and projection operator theory, which can dramatically reduce the sampling effort for learning the input-output behavior of high dimensional systems.

### **1.5.1 Meta-modelling Methods**

Meta-models can govern any of the physical parameters present in the real-world problems. Nevertheless, the precision of the meta-model should be enhanced to reflect the real system and simulate the performance of a product or system, which has the preferred design configuration and set of design parameters, by choosing a better



model. In general, the better the model is, the more accurate it represents the real system.

Some of the meta-modelling methods include gradient projection method (Kim and Na 1997; Alyanak et al. 2008), Rackwitz-Fiessler algorithms (Kim and Na 1997; Schanz and Salhotra 1992; Wu 1987), sensitivity analysis (Lee et al. 2011; Greerar and Manohar 2016; Wei et al. 2016; Schobi and Sudret 2019) which have been widely used in the uncertainty analysis. Also, these are popular in gathering needs of computationally demanding models in the uncertainty analysis. High dimensional model representation (HDMR) is one such technique developed for the parameter interaction in physical problems (Rabitz et al. 1999).

Despite the fact that several sampling techniques and various meta-model formation methods are readily available for use, the selection of suitable meta-modelling technique is the key concern in choosing the efficient one among the existing fracture analysis approaches. Since the entire sampling approaches and meta-modelling techniques have their unique properties, no universal meta-model is considered as a best choice for all types of problems. Therefore, the sampling method and meta-modelling technique for a specific type of problem has to be decided based on the degree of model complexity, existence of error in sample data, type and extent of input variables, anticipated level of precision and computational effectiveness. Table 1.1 summarises the different meta-modelling methods and sampling techniques applicable for reliability analysis studies. Furthermore, the sampling techniques and particular meta-modelling methods shown in Fig. 1.5 can be adopted to choose best likely performance of each model.

### **1.5.2 High Dimensional Model Representation**

HDMR is a response surface method established as dimension reduction method for reliability analysis. This technique can dramatically reduce the sampling effort for learning the input-output behaviour of high dimensional systems by correlated functions. HDMR has been employed for structural damage identification, inverse reliability problems and cohesive zone models in finding crack propagation etc. Also, HDMR was incorporated in estimating reliability with random and fuzzy functions (Balu and Rao 2014), interval dependencies (Xie et al. 2017).

Hence there is a considerable interest in quantifying hybrid uncertainties in assessing the reliability of structural systems. Response surface methods facilitate meta-models to reduce the effort involved in analysing multidimensional systems. Therefore in the present work, HDMR technique is utilised for response surface generation and HDMR based uncertainty analysis is developed for estimating the structural reliability in the presence of various imprecise uncertainties.

Table 1.1 Meta-modelling techniques

Modeling Methods	Sampling Techniques
<ul style="list-style-type: none"> <li>➤ Polynomial Regression (PR)</li> <li>➤ High dimensional model representation (HDMR)</li> <li>➤ Polynomial chaos expansion (PCE)</li> <li>➤ Splines [linear, cubic]</li> <li>➤ Multivariate adaptive regression splines (MARS)</li> <li>➤ Gaussian process</li> <li>➤ Kriging</li> <li>➤ Radial basis functions (RBF)</li> <li>➤ Least interpolating polynomials (moving least square) (MLS)</li> <li>➤ Artificial neural network (ANN)</li> <li>➤ Group method of data handling - polynomial neural network (GMDH - PNN)</li> <li>➤ Knowledge base or decision tree</li> <li>➤ Support vector machine (SVM)</li> <li>➤ Weighted least squares regression</li> <li>➤ Best linear unbiased predictor (BLUP)</li> <li>➤ Multi-point approximation (MPA)</li> <li>➤ Sequential or adaptive meta modeling</li> <li>➤ Hybrid models</li> </ul>	<ul style="list-style-type: none"> <li>➤ Classic methods <ul style="list-style-type: none"> <li>• Factorial design</li> <li>• Central composite design (CCD)</li> <li>• Box-Behnken</li> <li>• Optimal designs</li> <li>• Plackett-Burman</li> </ul> </li> <li>➤ Space-filling methods <ul style="list-style-type: none"> <li>• Simple grids</li> <li>• Latin Hypercube (LH)</li> <li>• Sobol sequence</li> <li>• Orthogonal arrays (Taguchi)</li> <li>• Hammersley sequence</li> <li>• Uniform designs</li> <li>• Minimax and maximin</li> </ul> </li> <li>➤ Hybrid methods</li> <li>➤ Random or human selection</li> <li>➤ Importance sampling</li> <li>➤ Directional simulation</li> <li>➤ Discriminative sampling</li> <li>➤ Sequential or adaptive methods</li> </ul>

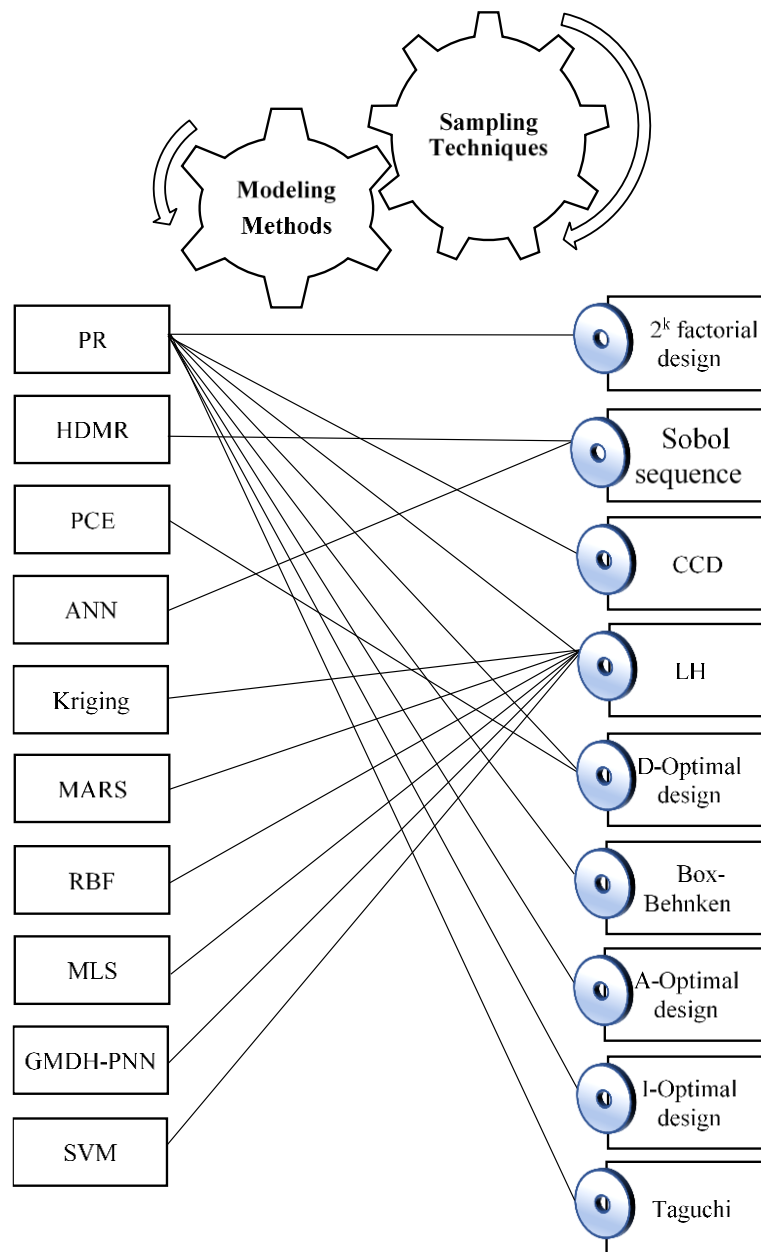


Fig. 1.5 Meta-modelling methods and corresponding sampling techniques

## **1.6 ORGANISATION OF THESIS**

The proposed methodology comprises, development of response surface by utilising HDMR, incorporating the imprecise uncertainties present in the structural systems in to the response surface, formulating the limit state function, and evaluating failure probability bounds. Also, modelling the system by FE and simulating the limit state function using different methods like MCS, FORM and SORM for comparing the accuracy and computational efficiency of the proposed methodology. Main objective of the study is to reduce the effort and achieve the accuracy efficiently in modelling the uncertainties and incorporating them into the high dimensional systems for finding the reliability.

The thesis is organised as follows:

- i. The first chapter describes a brief introduction to structural safety and reliability, methods for assessing structural reliability. Uncertainties, types of uncertainties, response surface methods and their importance in reliability analysis have also been discussed along with significance of the present work.
- ii. The second chapter presents a detailed review of relevant literature on structural reliability, uncertainties and surrogate models followed by summary of literature and objectives of the proposed research work.
- iii. The third chapter demonstrates the application of HDMR in uncertainty analysis. Numerical examples with p-box variables have been presented and the efficiency of the proposed methodology is compared with the conventional methods.
- iv. The fourth chapter exhibits reliability assessment of structural systems with hybrid uncertainties.
- v. The last chapter presents the conclusions based on the findings from the present work, and also scope for the future work.

## CHAPTER 2

### LITERATURE REVIEW

#### 2.1 GENERAL

The complex engineering structures are analysed by computer simulations, popular tool among them is finite element model based simulation. Due to inherent imprecise parameters present in the structures, direct FE simulation becomes inefficient to treat the imprecise parameters. In this context, some of the methodologies like, structural reliability analysis, robust design optimization and sensitivity analysis have gained attention in recent research work. Structural reliability analysis has acquired considerable recognition for risk and safety evaluation of engineering systems in past few decades. Methods of reliability analysis have been applied in multidisciplinary design environment, considering performance requirement, safety and serviceability of a system. They are broadly categorised as probabilistic (Beer et al. 2013; Melchers 2003; Sundgren et al. 2009; Zhang et al. 2019) and non-probabilistic methods (Faes and Moens 2019; Guo and Lu 2015; Li et al. 2016), depending on the input parameters. The input parameters such as loads, boundary conditions, geometrical and material properties for a system might be stochastic in nature, therefore it is utmost important to consider the variability of these input parameters. Due to insufficient or incomplete knowledge about the variability of input parameters, it is crucial to incorporate these imprecise parameters in estimation of reliability which contribute variability in the structural response. As the complexity of a system increases with increase in number of input parameters bearing variability, conventional simulation tools become inefficient and uneconomic. Hence, response surface methods or surrogate models (Balu and Rao 2012; Hajikolaie and Wang 2014; Lambert et al. 2016; Li et al. 2016; Xie et al. 2017) can be utilised in deriving mathematical formulation for an implicit system efficiently thereby reducing the effort involved in traditional simulation methods. A detailed literature study has been carried out on the structural reliability, imprecise uncertainties and surrogate models as a part of present work.

## 2.2 STRUCTURAL RELIABILITY

Structural reliability is associated with formulation of performance function or limit state function for estimating the system response and failure probability as in Eq. (1.1). The limit state function can be divided as ultimate limit state and serviceability limit state function (Choi et al. 2007). The former method is related to complete collapse of a system or part of a system (for example; corrosion, fatigue, fracture etc.), in which, risk of life and financial losses occur, hence it should have lesser probability of occurrence. The latter method is associated with disruption of the system (for example; excessive deflection or displacement, vibration etc.).

Traditional reliability analysis requires probability distributions of all the uncertain parameters. Stochastic FE method (Faravelli 1989), FORM and SORM are some of the traditional methods used for probabilistic reliability estimation. However in many practical applications, the variation bounds can be only determined for the parameters with limited information. A probabilistic model for marine corrosion of steel was studied by considering nonlinear corrosion uncertainty (Melchers 2003). A reliability analysis was performed on random space without any nonlinear transformations of probabilistic constraints (Du 2008). The probabilistic approach has certain limitations for the complex structures, which lead to a larger error in the structural reliability calculation due to variability of the input data. In addition, only a certain range of uncertainties can be utilised which cannot define the inaccuracy of the data. Hence, non-probabilistic approach gained much attention in recent past.

Non-probabilistic approach considers the imprecise data about input parameters based on the representation of uncertainties. Guo and Lu (2015) presented a non-probabilistic reliability method by considering the bounded uncertainties, interval variables and convex-set models. A semi-analytic method for calculating the non-probabilistic reliability index was presented by Jiang et al. (2007). Non-probabilistic reliability-based design optimization and robust reliability design of structures with uncertain-but-bounded parameters were studied (Luo et al. 2009; Wang and Qiu 2009).

Apart from probabilistic and non-probabilistic reliability methods, time variant (Czarnecki and Nowak 2008; Hawchar and Soueidy 2015) and time invariant methods (Astroza et al. 2017; Becker et al. 2012) have also gathered attention in estimating reliability. Yao and Wen (1996) estimated reliability of structures subjected to time

variant loads with uncertain parameters. Response surface model was derived by fast integration technique, and sensitivity analysis was carried out for finding the effect of uncertain parameters on the system reliability. Mejri et al. (2011) investigated lifetime of ageing naval structures by predicting the durability. The study was focused on time varying factors, corrosion and adhesive damage of the naval structures.

Sundar and Manohar (2014) presented time variant reliability analysis of nonlinear vibrating systems with random parameters in which Monte Carlo variance reduction strategy which was based on Girsanov transformation was introduced. Zhao et al. (2014) evaluated dynamic structural reliability on considering time variant parameters by moment method for a pre-stressed concrete containment. Wang and Chen (2016) utilised the limit state surrogate model to tackle the time independent systems by translating the random processes and time parameter into random variables. The surrogate model was updated using maximum confidence enhancement sequential sampling scheme.

Astroza et al. (2017) evaluated the time independent reliability using Bayesian methods. A framework was presented to identify the non-linear behaviour of structures due to seismic loading. Bayesian approach has widely been used in engineering fields to obtain balanced estimation by combining prior information with the observed data (Zhu and Frangopol 2013). Becker et al. (2012) utilised Bayesian sensitivity analysis for nonlinear systems. Stochastic analysis has been performed on systems for dynamic loading. Dey et al. 2016 presented the natural frequency analysis on laminated composite curved panels for practical application of noise induced effects and the study has been extended to stability analysis under non-uniform dynamic loading (Dey et al. 2018).

### **2.3 IMPRECISE UNCERTAINTY**

Uncertainties are inevitable in every system due to direct or indirect influencing sources. The uncertain parameters are conventionally calibrated by probability theory, which characterises the variability of a parameter by a single measure. But, with limited information on the uncertainty, it is very difficult to construct precise probability distributions for some imprecise parameters in many practical applications. Imprecise uncertain parameters are generally expressed in lower and upper bounds over a range of values (Crespo et al. 2013; Guo and Lu 2015; Liu et al. 2017; Wang et al. 2018; Wei

et al. 2019). Various approaches such as evidence theory (Feng et al. 2012; Yang et al. 2017), convex models (Liu and Zhang 2014; Wang et al. 2014), interval analysis (Jiang et al. 2012; Wu et al. 2017), fuzzy sets (Balu and Rao 2011; He et al. 2015), p-box (Simon and Bicking 2017; Schobi and Sudret 2017; Schobi and Sudret 2019), etc. have been developed to quantify imprecise uncertainties in the analysis of structural systems so far. These approaches differ from one another by the way the incomplete knowledge is interpreted/described thereby the type of mathematical propagation of the uncertainty. Also, these theories need the description of variables in bounds rather than precise information of probability distribution.

Evidence theory also called Dempster-Shafer theory or belief functions theory, is a convenient framework for modelling imperfect data. It is mainly used to define belief and plausibility for decision making. Belief functions naturally blend probabilistic and interval parameters (Simon and Bicking 2017). Convex models are generally represented as ellipsoidal models or interval models (Liu and Zhang 2014). Interval approach was first introduced by Ben-Haim and Elishakoff (1990) and further developed by many other researchers. Interval arithmetic can be applied for solving the mathematical problem, especially FE formulation of any system using interval FE concept with bounded parameters. Element-by-element technique was used to tackle the overestimation and compatibility condition using penalty method (Muhanna et al. 2007). Sundgren et al. (2009) demonstrated probabilistic networks for the study of imprecise probabilities. Effect of order of distributions on interval probabilities were investigated, and found that, for the wider intervals, the second order distribution is wrapped towards lower bound, thereby losing the most of the data about the uncertainty. Zhang et al. (2010) modelled uncertain parameters by interval bounds constructed from confidence intervals. Both epistemic and aleatory uncertainties were generated separately, and interval FE method was utilised to estimate the ranges of structural responses. Jiang et al. (2011) developed a technique based on the hybrid uncertainties present in the structural systems. The uncertainties were modelled as random fields and intervals. Reliability index approach (RIA), and performance measurement approach (PMA) were introduced based on the hybrid reliability models. Also, a monotonicity analysis was adopted to formulate algorithms for solving RIA and



PMA based reliability models. These efficient algorithms were introduced as replacement for low efficient two layer optimization.

Han et al. (2014) developed a hybrid reliability method to compute the failure probability of the structure due to probability interval hybrid uncertainty. In their study, a response surface was constructed using quadratic polynomial and a modified axial experimental design method. Liu et al. (2016) explored the impact of epistemic uncertainties on the reliability assessment. An adaptive surrogate model was developed for optimizing the multi-dimensional intervals by defining the width of interval as an objective function. The framework was set to find the lower value of reliability for multi-dimensional intervals. In the context of imprecise probability, the structural reliability bounds have been evaluated by considering imprecise measurements for concrete structure in FE model updating by Biswal and Ramaswamy (2017). Muscolino and Sofi (2017) presented interval analysis to limit the dependency overestimation, by applying improved interval analysis via extra unitary interval. Wang et al. (2018) estimated the reliability of systems subjected to imprecise probabilistic information by linear programming optimization. Two objective functions were formulated for calculating failure probability bounds, which were tighter compared to bounds obtained by interval MCS. Failure probability functions subjected to rare failure events with hybrid uncertainties were presented by Wei et al. 2019.

$\underline{P}(E)$  and  $\bar{P}(E)$  are a generalized representation of lower and upper probabilities of an event  $E$  respectively, with  $0 \leq \underline{P}(E) \leq \bar{P}(E) \leq 1$  for any imprecise variable. To handle imprecise uncertainties, interval analysis is unified with traditional probability theory, called probability bounds analysis, which is generally represented as p-box. P-box is a general representation of uncertainty, it can model epistemic and aleatory uncertainty on parameters by a family of probabilities (Simon and Bicking 2017). The propagation mechanism of p-boxes through mathematical functions was given by Ferson et al. (2002). P-box is a convenient representation of imprecise uncertainty, which ensemble lower and upper bounds of a quantity on its cumulative distribution function (CDF). The p-box approach renders a rigorous way to account for uncertainty for unknown dependence of random variables (Xiao et al. 2018). Karanki et al. (2009)

presented a novel probabilistic safety assessment based on probability bounds approach by unifying interval arithmetic and probability theory in constructing p-box.

It can be constructed with incomplete information about the probability distribution of a parameter regardless of the dependency. Zhang et al. (2013) presented construction of p-box by four different approaches, i.e., Kolmogorov-Smirnov confidence limits, bounded one-sided Chebyshev's inequality, Confidence interval on the mean value and the envelop of five candidate distributions. Out of these four, confidence interval p-box gives the most reasonable reliability assessment. They developed quasi-Monte Carlo method for reliability analysis for p-boxes, and also randomised variance-type error was estimated which replaced the pseudo random numbers by the low-discrepancy sequences. Guimaraes et al. (2018) adopted confidence interval of reliability estimates based on bootstrapping technique.

Crespo et al. (2013) utilised p-box in a reliability analysis framework for mechanical structure design that depends polynomially on uncertain parameters. Xiao et al. (2016) analysed the structural system with uncertain parameters which are modelled by p-boxes. Both load and material uncertainties were handled using non Monte Carlo p-box approach. Matrix decomposition strategy and fixed point formulation were utilised to reduce the over estimation of bounds. Schobi and Sudret (2017) utilized free and parametric p-boxes along with Kriging meta-models with adaptive experimental designs for estimating the probability of failure. Liu et al. (2017) developed intergeneration projection genetic algorithm for reliability assessment comprising p-box and random variables. Zhang et al. (2017) investigated application of p-box variables on the multiple dependent competing failure processes in predicting the reliability. An efficient method, dimension-reduced sequential quadratic programming was developed for the construction of p-box. Zhang et al. (2018) proposed a novel hybrid reliability analysis comprising p-box with fuzzy variables for turbine discs.

Computation of reliability index or failure probability becomes burdensome and impractical for the multi-dimensional systems comprising insufficient data or uncertainty. On incorporating p-box approach in reliability assessment to represent imprecise uncertainties, significantly better bounds on system responses can be obtained. Therefore, p-box approach is prominently adopted to construct imprecise

uncertainties and the effect of p-boxes on structural systems along with other sources of uncertainties has been studied in the present work.

## **2.4 SURROGATE MODELING**

High dimensional systems are cumbersome for the computation of reliability. Therefore, RSMs have been adopted which facilitates surrogate models or meta-models to reduce the effort involved during the simulation. Surrogate models enable approximation of implicit systems by deriving limit state or performance function, by facilitating the computational efficiency with accuracy. Some of the surrogate models like; polynomial regression (Bucher and Most 2008), polynomial chaos expansion (Xu and Kong 2018), Kriging (Echard et al. 2013; Yang et al. 2017), HDMR (Rabitz et al. 1999; Valko et al. 2017) and many more, to identify the possible failure events. These methods require sampling of the input parameters in-order to derive the response surface. Latin hypercube (Dolšek 2012; Giunta et al. 2006), Sobol sequence (Balesdent et al. 2016; Lambert et al. 2016), importance sampling (Echard et al. 2013; Murangira et al. 2015), sequential or adaptive methods (Lee et al. 2011) are generally used for sampling the input parameters.

Polynomial chaos expansion (PCE) facilitates random variables in an infinite series for higher order polynomial functions. This deters modelling of highly nonlinear systems in which the order of polynomial function increases and makes the model expensive and inaccurate. Hawchar et al. (2015) utilised PCE for addressing time-variant parameters in reliability analysis. Xu and Kong (2018) proposed a cubature collocation based sparse PCE for efficient structural reliability analysis.

Wang and Wang (2013) presented nested extreme response surface for time-variant reliability assessment by employing Kriging model. Yang et al. (2015) developed a method combining Kriging model with optimisation based interval Monte Carlo simulation (OIMCS). Since the Kriging model only predicts sign of the performance rather than the specific value which is needed for accurate results, a new method, active learning Kriging (ALK) was introduced for getting bounds of the failure probability. Li et al. (2017a) utilised Kriging based surrogate model for non-probabilistic reliability assessment with interval parameters by belief and plausibility measures. Although Kriging based meta-models are desired for approximating expensive black-box simulations, these snag by allowing exponential growth of training

samples as the dimensionality of the system increases. Ulaganathan et al. (2016) developed gradient enhanced Kriging surrogate by reducing the number of samples, which is more efficient than Kriging based meta-model.

The application of antecedently mentioned theories is restricted, since they are computationally burdensome to adopt for high dimensional complex structural models. Cost of performing such analyses is uneconomic which is directly proportional to complexity of the structure, type of analysis, and uncertainty conditions. In order to overcome these rigorous methods, HDMR was introduced by Rabitz et al. (1999).

HDMR expansions are attractive for representing functions with large number of input variables (Rabitz et al. 1999). The technique HDMR, basically facilitates lower-dimensional approximation of the original high-dimensional implicit function. Thereby, response surface generation of HDMR component function, can be simulated using simulation methods like MCS for computing the failure probabilities.

Various forms of HDMR can be constructed for different purposes such as ANOVA-HDMR (Li et al. 2000), Cut-HDMR (Xie et al., 2017) and RS-HDMR (Random sampling HDMR) (Rao and Balu 2018), adopted depending on the requirement in finding the component function. ANOVA-HDMR measures the contributions of the variance of each component functions to the overall variance of the output, while the cut-HDMR specifically exhibits the output  $g(\mathbf{X})$  in the hyperplane passing through a reference point  $\mathbf{c} = \{c_1, c_2, \dots, c_N\}$  defined in the variable space. RS-HDMR facilitates random sample points along with linear combination of basic functions (Hajikolaie and Wang 2014; Wei et al. 2019).

Kaya et al. (2004) presented a recursive algorithm for computing HDMR component functions individually which also calculates sensitivity indices. Chowdhury et al. (2008) utilized HDMR to explore the potential of the tool for tackling univariate and multivariate piece-wise continuous function. Ziehn and Tomlin (2009) developed an extended RS-HDMR, a surrogate model, which utilises graphical user interface (GUI). This surrogate model also performs efficiently in finding variance based sensitivity indices. Indexing HDMR (I-HDMR) was proposed by Tunga (2011) for multivariate interpolation systems with random fields. An adaptive support vector regression (SVR) was utilised along with HDMR by Xiong et al. (2012) for nonlinear

models. Mukhopadhyay et al. (2015) introduced an efficient hybrid method based on RS-HDMR and GA with unconstrained multivariable function. The application of HDMR in stochastic multi-scale modeling in conjunction with multi-element least square approach was carried out by Jiang and Li (2015). Concept of SVR was utilised in computing the sensitivity indices with an adequate number of sample points in accordance with HDMR (Li et al. 2017b). Jha and Li (2017) combined HDMR and artificial neural network (ANN) for estimating failure probability in presence of random variables. Naveen and Balu (2017) presented a genetic algorithm (GA) with HDMR for structural damage identification in large structures by finite element model updating. Principle component analysis combined with HDMR (PCA-HDMR), was proposed by Hajikolaie and Wang (2017) for finding coefficients that provide linear combination without using integrals.

In recent years, the research is extended for the application of HDMR to non-probabilistic uncertainty analysis. Fuzzy analysis for implicit and explicit functions were developed (Balu and Rao 2012a; b) using integrated finite element modelling and HDMR based response surface generation. The uncertainties involved in the systems were modelled as fuzzy variables and random variables. The study was extended to get the explicit expression without derivatives of response function with respect to uncertainties. Fast Fourier Transformation techniques were used to obtain the unknown design parameters in inverse reliability analysis (Balu and Rao 2013).

Xie et al. (2017) considered hybrid uncertainties consisting of dependent interval variables and random variables for the reliability analysis. Due to dependent intervals, the evaluation of reliability for every pair of dependent intervals, need nested double-loop procedure. This makes the analysis inefficient, hence to increase the efficiency, cut-HDMR was utilised, with leave-one-out sampling strategy.

There is a considerable interest for HDMR based uncertainty analysis with uncertainty other than intervals and fuzzy variables. Therefore, in present work, HDMR is utilised for deriving surrogate model with p-box uncertainties.

## 2.5 SUMMARY OF LITERATURE REVIEW

Structural reliability is estimated with respect to performance or limit state function. Simulation techniques are necessary to estimate the probability of failure when analytical approaches are impractical. Complicated large engineering systems are expected to have multiple number of uncertain variables. Such complex structures, cannot be analysed only by simulations. To minimise the number of performance function computations and to get the accurate estimation of failure probability, meta-modelling or surrogate modelling techniques are used. Many researchers in the past have focused on the improvements with respect to the computational efficiency in the reliability and risk management. Extensive review has been made on RSMs in presence of uncertainties in terms of Dempster Shafer evidence theory, random set theory, fuzzy set theory or p-box variables.

- Only a limited amount of research has been carried out for meta-modelling of the structural systems in presence of p-box uncertainties. Similarly efficient surrogate model suitable for the imprecise probability descriptions are hardly present in the literature.
- In order to address the severity in the systems having large inputs, an approximation technique called HDMR has been developed to study the input-output relationships of the system. The concepts of HDMR have been extensively implemented in uncertainty analysis when the input uncertain variables are random or fuzzy. However the practical description of uncertainties by means of p-box is not explored in the context of computational efficiency using HDMR techniques.
- In many situations, the sources of uncertainties may not be same, hence the hybrid nature of uncertainties is inevitable. Only a limited studies have been conducted in the context of hybrid uncertainties, for example interval & random, and fuzzy & random. The hybrid nature among p-box, random variables, interval and fuzzy variables is not explored in the literature so far for the estimation of structural responses and structural reliability.
- From the literature study, the proposed research addresses the application of efficient meta-model techniques in the uncertainty analysis of structures when the uncertain variables are described as p-box.

## **2.6 RESEARCH OBJECTIVES**

The objectives of the present research work are as follows:

- i. To study the uncertainty analysis of the structures with imprecise uncertain parameters using HDMR.
- ii. To estimate the reliability of structures with p-box uncertain variables by interval Monte Carlo method.
- iii. To evaluate the reliability of structures in presence of hybrid uncertain variables.

## **2.7 SCOPE OF PRESENT RESEARCH**

- i. To model the uncertain parameter as p-box based on the available imprecise data for a given structure.
- ii. To develop HDMR based approximation function for a given structure with uncertainties.
- iii. To evaluate bounds on response of the system, and thereby failure probability bounds according to corresponding threshold limits by static analysis method.
- iv. To determine bounds on failure probability for hybrid uncertainties.
- v. To verify the results obtained from proposed HDMR based uncertainty analysis with conventional methods like interval Monte Carlo Simulation.





## CHAPTER 3

### HDMR BASED UNCERTAINTY ANALYSIS

#### 3.1 UNCERTAINTY ANALYSIS

Uncertainty analysis investigates the knowledge based uncertainty of a parameter which is knowledge based by quantifying with relevant available data. Uncertainty quantification emphasis characterisation and reduction of uncertainties in computational analysis. The method allows to determine the possible outcomes of a system with insufficient quantities which regulate the outcome. Most of the engineering systems rife with sources of uncertainties, which may arise in various context in different stages of experiments or mathematical modelling. Fig. 3.1 shows some of the sources of uncertainties, and corresponding description is stated in Table 3.1.

Uncertainty quantification is intended to treat and/or reduce the uncertainties. For aleatory uncertainties, quantification is relatively straightforward. Techniques like Monte Carlo method is generally used in this case, where probability distribution of variables are given by moments (i.e., mean and standard deviation), wherein quantifying epistemic uncertainties is tedious in which efforts are made to gain better knowledge about the uncertainty. Probability bounds analysis, fuzzy logic, evidence theory, Dempster-Shafer theory or Bayesian theory are used in quantification of epistemic uncertainties. SVR based uncertainty quantification in conjunction with Latin hypercube sampling was developed (Dey et al. 2016).

Irrespective of type of uncertainty, quantification can be done in two ways, firstly forward propagation and secondly inverse propagation (Faes and Moens 2019). In forward propagation of uncertainty, various sources of uncertainty is disseminated in predicting the system response through a model. This method focused on influence of parametric variability on the output. In inverse method of quantification, parameter uncertainty is calibrated and estimation of discrepancy between mathematical model and experimental results.

Table 3.1 Description of sources of uncertainties

SOURCES	DESCRIPTION
Parameter uncertainty	Arises due to errors in computer models or mathematical models, whose physical values are unknown and insufficient to perform experiments.
Parametric variability	The variability in input parameters due to manufacturing defects (material property and dimensions) which in turn affects the performance of the system.
Structural uncertainty	Refers to model discrepancy, which arises due to lack of knowledge about the system parameters in mathematical modelling. This accumulates errors in mathematical model consisting of defective or ambiguity input parameters.
Algorithmic uncertainty	Arises due to numerical errors and approximations in modelling the system.
Experimental uncertainty	An observational error arises in experimental measurements.
Interpolation uncertainty	If simulation results are insufficient, the data generated should be interpolated or extrapolated in predicting the responses.

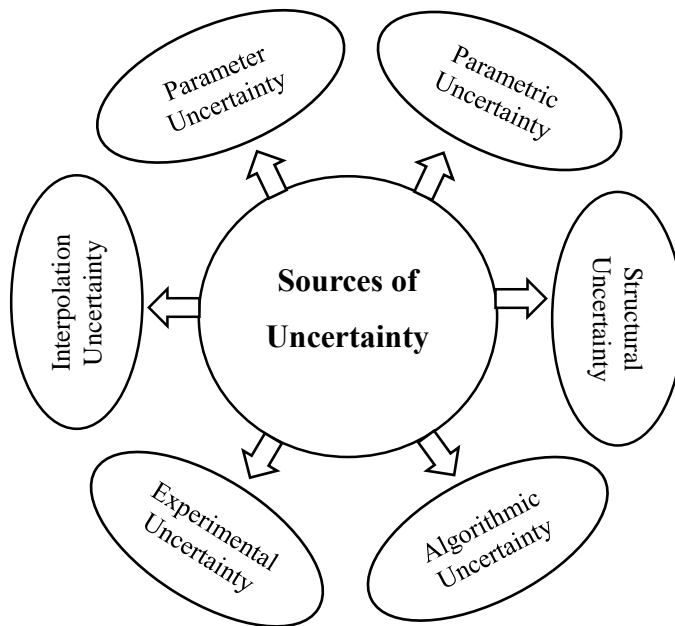


Fig. 3.1 Sources of uncertainties

Forward uncertainty propagation includes probabilistic and non-probabilistic approaches. Probabilistic methods are rigorous to perform as the random variability is considered in forming joint PDF of various parameters present in the system under consideration, some of the methods are mentioned as,

- Simulation based methods: Monte Carlo simulations, importance sampling, adaptive sampling, etc.
- Local expansion-based methods: Taylor series, perturbation method, etc.
- Functional expansion-based methods: Neumann expansion, orthogonal or Karhunen-Loeve expansions (KLE), polynomial chaos expansion (PCE) etc.
- Most probable point (MPP) based methods: First-order reliability method (FORM) and second-order reliability method (SORM).
- Numerical integration-based methods: Full factorial numerical integration (FFNI) and dimension reduction (DR) methods.

Non-probabilistic approaches include, interval analysis, Fuzzy theory, possibility theory, evidence theory and probability-box approach etc.

Inverse uncertainty propagation includes majorly Bayesian approach and regression analysis which require lesser subjective information on the imprecise probability.

### 3.1.1 Failure Probability and Reliability Index

Reliability analysis evaluates the failure probability of structural systems by determining whether the limit state function is exceeding the threshold value or not.

Considering a simple structure, suppose,  $Y$  is the resistance/strength of the structure, and  $W$  is the action/load effect (force or displacement response) on the structure, its failure criteria is defined as,

$$\begin{aligned} P_f &= P(Y < W) \\ &= P(Y - W < 0) \end{aligned} \tag{3.1}$$

Reliability index and failure probability is derived for the two cases, as mentioned below:

*Case 1:* On assuming  $Y$  as a random variable, with PDF of  $f_Y(y)$  and  $W$  to be deterministic, failure probability is expressed as in Eq. (3.2) and is shown in Fig. 3.2.

$$P_f = \int_{-\infty}^w f_Y(y) dy \quad -\infty \leq y \leq \infty \quad (3.2)$$

Case 2: if both  $Y$  and  $W$  are random variables, the PDF of both  $Y$  and  $W$  are shown in Fig. 3.3. The shaded portion in figure, indicates failure probability and is computed as follows:

Assuming, the probability density of  $W$  as  $w$ , and the area  $A_1$ , as shown in Fig. 3.4, where  $Y > w$  is equal to the shaded area  $A_2$  under the density  $Y$ .

Therefore,

$$P\left(w - \frac{dw}{2} < W < w + \frac{dw}{2}\right) = f_W(w) dw = A_1 \quad (3.3)$$

$$P(Y > w) = \int_w^{\infty} f_Y(y) dy = A_2 \quad (3.4)$$

When  $W$  takes the value  $w$ , reliability is the product of these two probabilities in Eqs. (3.3) and (3.4),

$$dR = f_W(w) dw \int_w^{\infty} f_Y(y) dy \quad (3.5)$$

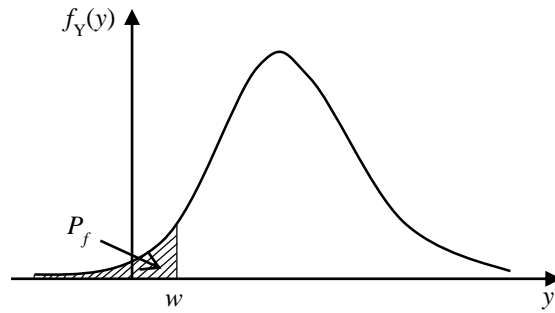


Fig. 3.2 Failure probability of deterministic strength of structure ( $Y$ )

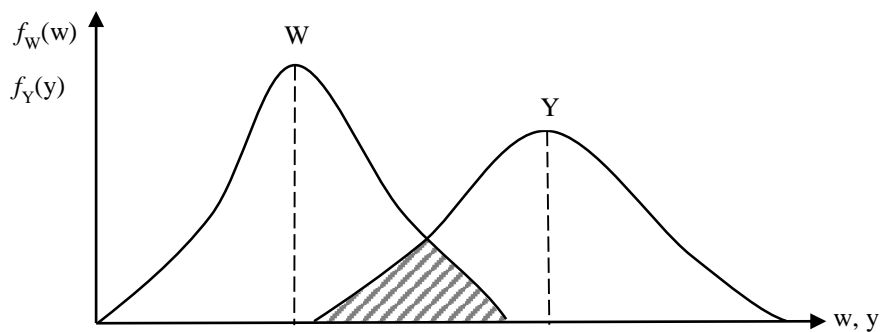


Fig. 3.3 Failure probability of strength ( $Y$ ) and load effect ( $W$ )

In other words,  $R$  is the probability of  $Y$  being greater than all possible values of  $W$ ,

$$R = \int dR = \int_{-\infty}^{\infty} f_W(w) \left[ \int_w^{\infty} f_Y(y) dy \right] dw \quad -\infty \leq w \leq \infty \quad (3.6)$$

Generally, limit state indicates the margin of safety between resistance ( $Y$ ) and loading ( $W$ ) of the structure under consideration. Therefore,  $g(\mathbf{X})$  is expressed as the function of  $Y$  and  $W$ , and according to the definition of limit state function, failure probability is defined as,

$$g(\mathbf{X}) = Y(\mathbf{X}) - W(\mathbf{X}) \quad (3.7)$$

$$\begin{aligned} P_f &= P[(Y(\mathbf{X}) - W(\mathbf{X})) < 0] \\ &= P[g(\mathbf{X}) \leq 0] \end{aligned} \quad (3.8)$$

where  $Y$  and  $W$  are the function of random variables. Such that,  $g(\mathbf{X}) \leq 0$  denotes failure region,  $g(\mathbf{X}) = 0$  and  $g(\mathbf{X}) > 0$  denote limit state surface and safe region respectively, as shown in Figs. 1.1 and 1.2.

If the mean and standard deviation of  $g(\mathbf{X})$  are denoted as  $\mu_g$  and  $\sigma_g$  respectively, then by definition, it is the difference of the mean and standard deviation of  $Y$  and  $W$ , i.e.,

$$\mu_g = \mu_Y - \mu_W \quad (3.9)$$

$$\sigma_g = \sqrt{\sigma_Y^2 + \sigma_W^2 - 2\rho_{YW}\sigma_Y\sigma_W} \quad (3.10)$$

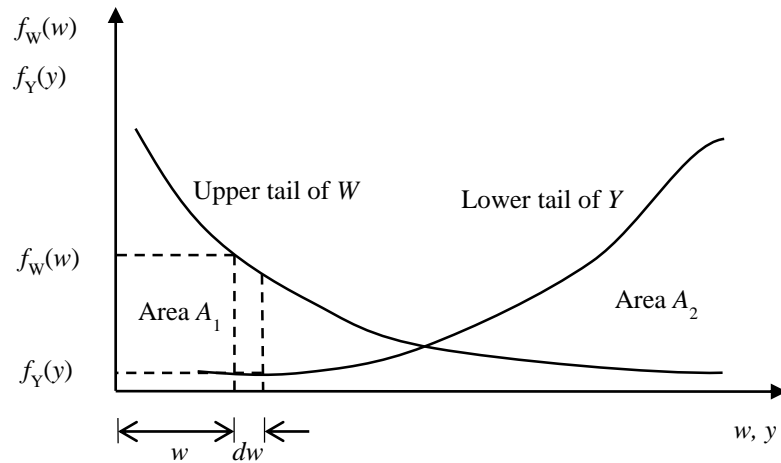


Fig. 3.4 Concept of reliability

where  $\rho_{YW}$  is the coefficient of correlation between  $Y$  and  $W$ . The safety index or reliability index  $\beta$  is defined as,

$$\beta = \frac{\mu_g}{\sigma_g} = \frac{\mu_Y - \mu_W}{\sqrt{\sigma_Y^2 + \sigma_W^2 - 2\rho_{YW}\sigma_Y\sigma_W}} \quad (3.11)$$

If  $Y$  and  $W$  are uncorrelated ( $\rho_{YW} = 0$ ), reliability index is expressed as,

$$\beta = \frac{\mu_g}{\sigma_g} = \frac{\mu_Y - \mu_W}{\sqrt{\sigma_Y^2 + \sigma_W^2}} \quad (3.12)$$

If  $Y$  and  $W$  are assumed to be normally distributed and uncorrelated, and the limit state function  $g(\mathbf{X})$  is also normally distributed, then, PDF of  $g(\mathbf{X})$  is expressed as,

$$f_g(g) = \frac{1}{\sigma_g \sqrt{2\pi}} \exp \left[ -\frac{1}{2} \left( \frac{g - \mu_g}{\sigma_g} \right)^2 \right] \quad (3.13)$$

Hence the failure probability is evaluated as,

$$P_f = \int_{-\infty}^0 f_g(g) dg \quad (3.14)$$

If,  $g(\mathbf{X}) = 0$  (normally distributed), the failure probability is computed as,

$$\begin{aligned} P_f &= \int_{-\infty}^0 \frac{1}{\sigma_g \sqrt{2\pi}} \exp \left[ -\frac{1}{2} \left( \frac{0 - \mu_g}{\sigma_g} \right)^2 \right] dg \\ &= \int_{-\infty}^0 \frac{1}{\sigma_g \sqrt{2\pi}} \exp \left( -\frac{1}{2} \beta^2 \right) dg \\ &= 1 - \Phi(\beta) \\ &= \Phi(-\beta) \end{aligned} \quad (3.15)$$

where,  $\Phi$  is standard normal cumulative distribution function. For the multi-dimensional case, the generalised Eq. (1.3) becomes,

$$P_f = P[g(\mathbf{X}) \leq 0] = \int \dots \int f_{\mathbf{X}}(x_1, x_2, \dots, x_N) dx_1 dx_2 \dots dx_N \quad (3.16)$$

Computation of failure probability as in Eq. (3.16) is applicable for aleatory uncertainties with corresponding distributional parameters and PDF. However, it is challenging to estimate failure probabilities in presence of imprecise uncertainties. Hence the reliability analysis demands the exploration of entire domain of bounds on imprecision in input variables.

### 3.1.2 Probability-box

Imprecise probability analysis distinguishes the well-known probability theory by probability bounds analysis for uncertainties with bounds. Probability bounds analysis is combination of interval analysis and probability theory, and the uncertainty is stated as, probability-box (p-box). P-box describes an ambiguous quantity with lower and upper bounds as a unified mathematical model to describe uncertainties with imprecise dependencies. Bounds on the parameter can be obtained from interval arithmetic functions (Chakraborty et al. 2017) and optimization methods (Liu et al. 2017). Efficiency of arithmetic functions is higher than that of the optimization methods but bounds are wider than the actual, which in turn results in overestimation. To overcome these overestimation, some of the techniques have been developed are Taylor series expansion method and Chebyshev interval method (Wu et al. 2017).

P-box can be constructed in various aspects on the basis of available insufficient data about a quantity as,

- i. Distributional p-box or parametric p-box: P-box whose probability parameters are specified indefinitely as intervals with known shape (i.e., normal, uniform, beta, weibull, etc.). Bounds of the p-box are enclosed by extreme values of distributions in terms of mean and standard deviation of the given parameter.
- ii. Distribution free p-boxes or free p-box: P-box whose mean and standard deviation is known, but distribution family is unknown. Here there is no assumption of shape or family of distribution but bounds are enclosed significantly when distribution is considered as unimodal. Distributions which match the given moments can be considered by some inequalities such as Markov, Chebyshev, etc.
- iii. P-boxes from imprecise measurements: When random sample data are ample, the empirical distributions can be used for calculating the values with significant measurement uncertainty represented by ranges about the sample, as p-box.
- iv. Confidence bands: If probability is designated by confidence bands, it is required to select the confidence level less than 100% for the result to be non-vacuous. They will completely enclose the distribution from which the

data were randomly sampled. A confidence band about a distribution function is sometimes used as p-box even though it represents statistical data rather than rigorous or sure bounds.

- v. Envelopes of possible distributions: P-box can be constructed as the envelope of various cumulative distributions, as a variable can be described by multiple probability distributions.
- vi. P-boxes from calculation results: P-box can arise from computations involving probability distribution or involving both a probability distribution and an interval, or involving other p-boxes.

P-box approach has been used in many fields specially in engineering and environmental science. Some of the applications are mentioned below:

- Reliability and risk assessment in structural engineering
- Sensitivity analysis in aerospace engineering
- Groundwater modelling
- Uncertainty propagation for salinity risk models
- Engineering systems for drinking water treatment, and heavy metal contamination in soil
- Safety assessment of power supply system
- Some of the applications other than engineering disciplines are, human health, endangered species assessment, agriculture, water pollution, cost estimates, weather forecasting, groundwater pollution, etc.

### 3.1.3 Construction of p-box

Consider a p-box variable defined as,  $x = [\underline{x}, \bar{x}]$ , with  $\underline{x}$  as lower bound and  $\bar{x}$  as upper bound within the interval. Let the CDF,  $F(x)$  for a random variable  $X$  lies in the space  $[0, 1]$ . For every  $x$ , an interval  $[\underline{F}(x), \bar{F}(x)]$  extensively is found to bound the possible values of  $F(x)$  as,

$$[\underline{F}(x) \leq F(x) \leq \bar{F}(x)] \quad (3.17)$$

such a pair of two CDFs constructs p-box. The expression for failure probability from MCS is given by,



$$P_f \approx \frac{1}{N_s} \sum_{k=1}^{N_s} I[g(x_k) \leq 0] = \begin{cases} 1, & \text{if } I[\cdot] \text{ is true} \\ 0, & \text{if } I[\cdot] \text{ is false} \end{cases} \quad (3.18)$$

where  $N_s$  is number of samples, and  $I[\cdot]$  is indicator function, and  $x_k$  is  $k^{\text{th}}$  simulated sample of  $X$ , which can be generated using inverse transform method.

$$x_k = F_X^{-1}(v_j) \quad j=1,2,\dots,N \quad (3.19)$$

where  $v_j$  is sample of random variable. If the variable  $X$  is not precisely defined with known PDF, then it may be assumed to fall in between two extreme ranges for the PDF. In this context, failure probability also varies in ranges  $[\underline{P}_f, \overline{P}_f]$ . This interval of failure probability can be evaluated using IMCS (Zhang et al. 2010) as expressed in Eqs. (3.20) and (3.21) which represent lower and upper bounds of failure probability respectively for all possible values of  $F(x)$ .

$$\underline{P}_f = \min \left\{ \frac{1}{N_s} \sum_{k=1}^{N_s} I \left[ g \left( F_X^{-1}(v_j) \right) \leq 0 \right] \right\} \quad (3.20)$$

and

$$\overline{P}_f = \max \left\{ \frac{1}{N_s} \sum_{k=1}^{N_s} I \left[ g \left( F_X^{-1}(v_j) \right) \leq 0 \right] \right\} \quad (3.21)$$

Similarly, for the response function  $g(\mathbf{X})$ , CDF intervals are defined as  $[\underline{g}, \overline{g}]$ . The lower and upper bounds of the interval are expressed as Eqs. (3.22) and (3.23) respectively,

$$\underline{g} = \min_{x \in [\underline{x}, \overline{x}]} \{g(\mathbf{x})\} \quad (3.22)$$

and

$$\overline{g} = \max_{x \in [\underline{x}, \overline{x}]} \{g(\mathbf{x})\} \quad (3.23)$$

For example, if  $X$  is a normal random variable with standard deviation of 0.5, and due to limited resource, mean of the variable is not precise and lies in an interval between  $[2, 3]$ , then the variable is modelled as p-box as shown in Fig. 3.5.

Cartesian product method is commonly adopted for computations involving p-boxes. Interval arithmetic is another way to compute with p-boxes, where numerical calculations for interval numbers are required, for example, interval finite element

method (IFEM). Elementary operations of real arithmetic can be extended to interval numbers also. Eq. (3.24) implies the arithmetic operation, where  $x$  and  $y$  are the generic elements, i.e.,  $x \in X$ ,  $y \in Y$ , and  $\circ \in \{+, -, \times, \div\}$ .

$$x \circ y = [\min x \circ y, \max x \circ y] \quad (3.24)$$

### 3.2 HIGH DIMENSIONAL MODEL REPRESENTATION

Computational complexity in generating a multivariate function increases as the number of input variables increases for conventional methods. HDMR is a tool established to capture multiple input-output relation of the system (Balu and Rao 2012a). Although multi-dimensional systems require higher order correlations in formulating system response, HDMR allows lower order terms to encompass the entire system response.

HDMR is a correlated function expansion which maps input-output in an orderly manner. Let  $g(\mathbf{X})$  be the response function with  $N$  input variables. The first-order HDMR expansion is defined as,

$$g(\mathbf{X}) = g_0 + \sum_{i=1}^N g_i(x_i) + \sum_{1 \leq i_1 < i_2 \leq N} g_{i_1 i_2}(x_{i_1}, x_{i_2}) + \dots + g_{12 \dots N}(x_1, x_2, \dots, x_N) \quad (3.25)$$

where  $g_0$  is a constant term representing the response at reference point  $\mathbf{c}$ . Here,  $g_i(x_i)$  is a first-order term indicating the effect of  $x_i$  acting alone. The function  $g_{i_1 i_2}(x_{i_1}, x_{i_2})$  is a second-order term which defines the interdependent effects of the variables  $x_{i_1}$  and

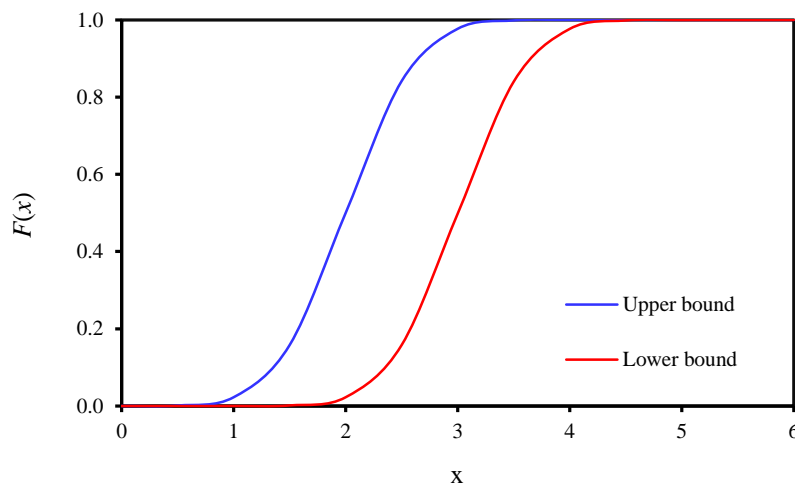


Fig. 3.5 P-box with a mean [2, 3] and standard deviation 0.5

$x_i$ , and  $g_{1,2,\dots,N}(x_1, x_2, \dots, x_N)$  represents any residual dependence of all the input variables, which shows the impact on the output  $g(\mathbf{X})$ . With all the component functions in Eq. (3.25), an efficient model can be derived which replaces an expensive implicit system without compromising accuracy. Based on the previous studies, it is witnessed that, first-order expansions are likely sufficient to characterise outputs of varied realistic systems.

Different forms of HDMR can be constructed for different purposes which are adopted depending on the requirement in finding the component function. ANOVA-HDMR allows the decomposition of a multivariate dependence into a hierarchical sum of terms with increasing dimensionality. The cut-HDMR expansion is an exact representation of the output in the hyperplane passing through a reference point in the variable space. The approximation contains contribution from all input variables. Thus, the infinite number of terms in the Taylor series is partitioned into finite different groups, and each group corresponds to one cut-HDMR component function. Therefore, any truncated cut-HDMR expansion provides a better approximation and convergent solution of  $g(\mathbf{X})$ . RS-HDMR is a practical procedure based on randomly sampled input variables. Evaluation of the high-dimensional integrals in the RS-HDMR expansion can be carried out by Monte Carlo random sampling. To reduce the sampling effort, the RS-HDMR component functions may be approximated by expansions in terms of a suitable set of functions, such as orthonormal polynomials, spline functions, or even simple polynomial functions.

In order to derive an exact output for given variable space, cut-HDMR method is utilised in the proposed research. To begin with, a reference point  $\mathbf{c} = \{c_1, c_2, \dots, c_N\}$  is chosen for an input vector  $\mathbf{X}$ , within the region of interest. Then, expansion functions are determined by using responses relative to the predefined reference point  $\mathbf{c}$ , all along the input variable space. Suppose  $N$  is the number of variables present in the system under consideration, and  $n$  is the number of sample points considered on the variable axes, then the number of function evaluations ( $N_s$ ) for any order is calculated (Rao and Chowdhury 2009) as,

$$N_s = \sum_{s=0}^k \frac{N!}{(N-1)!s!} (n-1)^s \quad (3.26)$$

where  $s$  is the order of the component function. On considering only up to first-order term, the component functions from Eq. (3.25) can be written as,

$$g_0 = g(\mathbf{c}) \quad (3.27)$$

$$g_i(x_i) = g(x_i, c_i) - g_0 \quad (3.28)$$

here,  $g_i(x_i, c_i) = g(c_1, c_2, \dots, c_{i-1}, x_i, c_{i+1}, \dots, c_N)$  which implies that, all the values of input parameters are at  $\mathbf{c}$  except  $x_i$ . Values of  $g_0$  at each point on the variable axes can be calculated by any existing analysis tool, like finite element method. Further, for  $x_i = x_i^j$  the function is defined for  $n$  sample points as,

$$g(x_i^j, c_i) = g(c_1, c_2, \dots, c_{i-1}, x_i^j, c_{i+1}, \dots, c_N) \quad j = 1, 2, \dots, n \quad (3.29)$$

The function is evaluated for each division on the variable space by interpolating the values using Lagrange's interpolation method, hence the component function  $g_i(x_i)$  from Eq. (3.29) is expressed as,

$$g(x_i^j, c_i) = \sum_{j=1}^n \phi_j(x_i) g(c_1, \dots, c_{i-1}, x_i^j, c_{i+1}, \dots, c_N) \quad (3.30)$$

where,  $\phi_j(x_i)$  is Lagrange's interpolation term for first-order, evaluated as,

$$\phi_j(x_i) = \frac{(x_i - x_i^1) \dots (x_i - x_i^{j-1})(x_i - x_i^{j+1}) \dots (x_i - x_i^n)}{(x_i^j - x_i^1) \dots (x_i^j - x_i^{j-1})(x_i^j - x_i^{j+1}) \dots (x_i^j - x_i^n)} \quad (3.31)$$

Similarly, all the remaining component functions should be generated so as to formulate the output function  $g(\mathbf{X})$ . On substituting  $g(x_i, c_i) = g(x_i^j, c_i)$  in Eq. (3.28) and adding Eqs. (3.27) and (3.28), the first-order approximation function  $\tilde{g}(\mathbf{X})$  can be obtained as,

$$\tilde{g}(\mathbf{X}) = \sum_{i=1}^N \sum_{j=1}^n \phi_j(x_i) g(c_1, \dots, c_{i-1}, x_i^j, c_{i+1}, \dots, c_N) - (N-1)g_0 \quad (3.32)$$

The HDMR is implemented in various disciplines such as, optimization, molecular physics, chemical kinematics, atmospheric models, etc. for failure and risk assessments, and uncertainty analysis. Also, mathematical models can be constructed

impressively by using laboratory or field data with lesser computational effort. The HDMR is utilised in deriving response function for linear as well as nonlinear systems (Naveen and Balu 2017; Rao and Balu 2019). Also, it has been applied to the uncertainty analysis with dependant intervals (Xie et al. 2017) and fuzzy variables (Balu and Rao 2014).

Based on the previous studies, it is witnessed that, the correlated functions in an HDMR expansion are optimal choices tailored to  $g(\mathbf{X})$  over the entire domain of  $\mathbf{X}$ , hence, the high order terms in the expansion are often negligible. Therefore, in this work, first-order HDMR expansions, which are likely sufficient to characterize outputs of varied realistic systems, is utilised in deriving the approximation function for various systems with imprecise uncertainties. Also, very small number of sample points should be avoided in HDMR approximation, as it may not capture the nonlinearity outside the domain of sample points and this in turn affects the estimated solution (Rao and Chowdhury 2009). The sampling scheme for a function having one variable ( $X$ ) and two variables ( $X_1, X_2$ ) is shown in Figs. 3.6 (a) and (b), respectively.

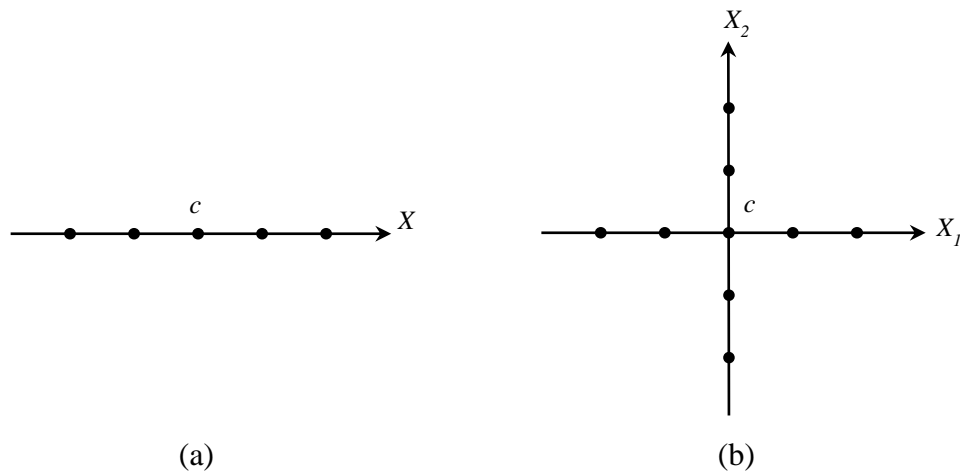


Fig. 3.6 Sampling scheme for first-order HDMR: (a) for a function with one variable ( $X$ ); and (b) for a function with two variables ( $X_1$  and  $X_2$ )

### 3.3 NUMERICAL EXAMPLES

The proposed HDMR based uncertainty analysis is verified for the efficiency and accuracy by applying to some of the explicit and implicit structural problems. Figure 3.7 shows the steps involved in first-order HDMR based uncertainty analysis. First two examples are presented to study the responses of the function with imprecise variables, and the rest of the examples demonstrate the efficiency in the reliability estimation. An exact continuous and approximated function obtained from the HDMR technique is simulated with IMCS for different function evaluations corresponding to various sample points and variation in the bounds of response of the models and failure probability is studied.

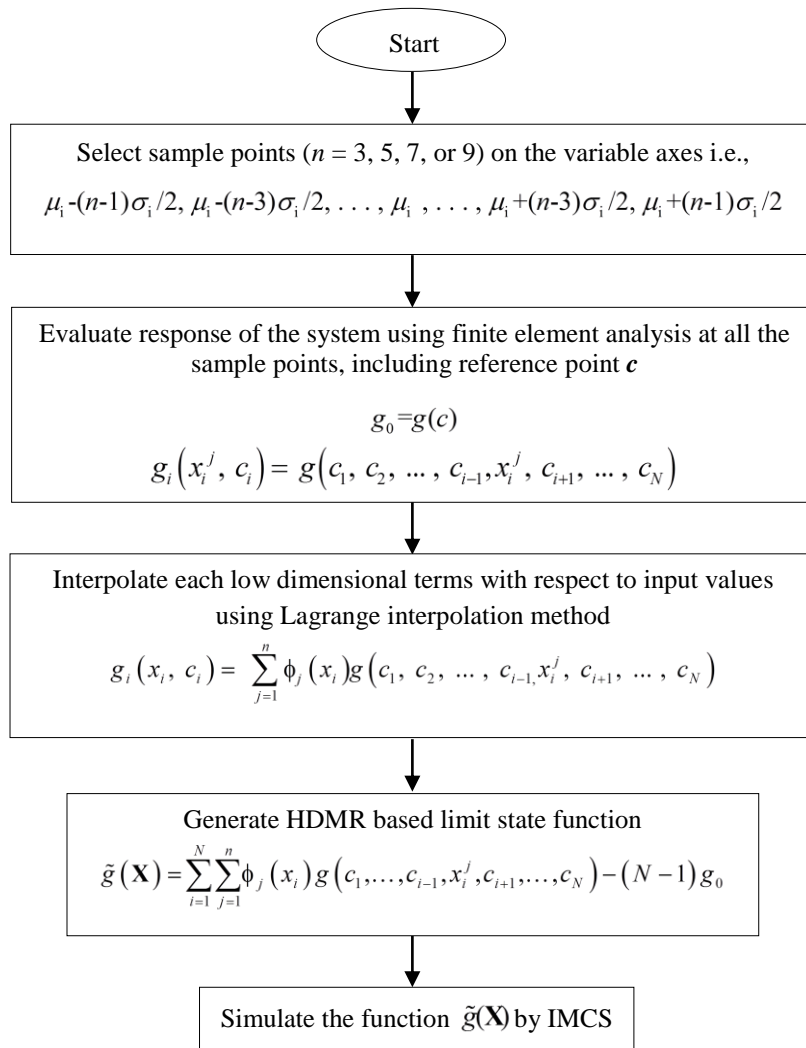


Fig. 3.7 Flowchart for the first-order HDMR based function.

### 3.3.1 Explicit Cubic Function

An explicit cubic function is considered (Chowdhury et al. 2009) as in Eq. (3.33) consisting of two normal independent p-box variables with interval mean [7.06, 12.94] and standard deviation 3.0.

$$g(\mathbf{X}) = 2.2257 - \frac{0.025\sqrt{2}}{27}(x_1 + x_2 - 20)^3 + \frac{33}{140}(x_1 - x_2) \quad (3.33)$$

The function  $g(\mathbf{X})$  is simulated using crude IMCS for 1,00,000 evaluations to obtain the response bounds. Then, the first-order HDMR is applied to obtain the approximated response function which replaces the function  $g(\mathbf{X})$  with computational efficiency. The number of sample points on p-box variables  $x_1$  and  $x_2$  have been varied from  $n=3$  to 7 for the parametric study. The response bounds are presented in Table 3.2, which are compared with the direct IMCS results. The corresponding CDF curves are shown in Fig. 3.8.

From Table 3.2, it is witnessed that sample point  $n=3$  is showing slight error in response bounds, wherein  $n=5$  is showing negligible error and  $n=7$  is nearing to the original model results with more accurate bounds. Hence CDF of HDMR curves are overlapping the CDF of original model in Fig. 3.8.

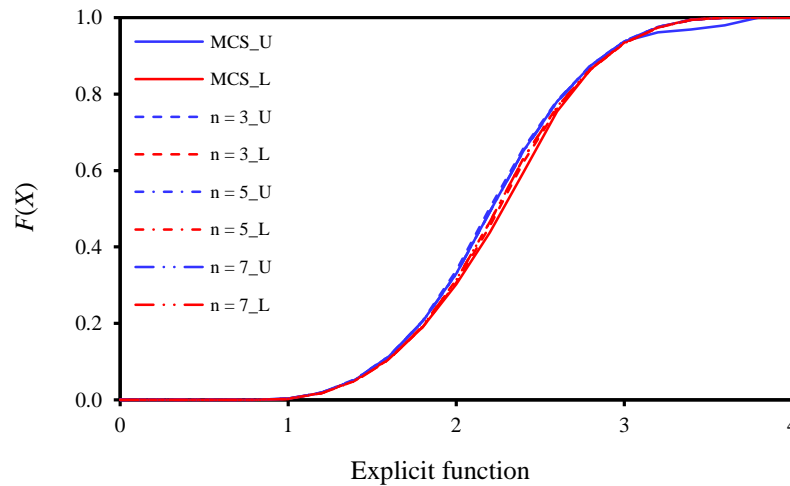


Fig. 3.8 CDF of explicit function in Eq. (3.33)

Table 3.2 Response bounds of explicit function in Eq. (3.33)

	Response		% Error		Effort	
	LB	UB	LB	UB	LB	UB
Direct IMCS	0.8405	3.6095	-	-	100000	100000
HDMR ( $n=3$ )	0.8526	3.6043	1.44	0.140	5	5
HDMR ( $n=5$ )	0.8430	3.6062	0.30	0.090	9	9
HDMR ( $n=7$ )	0.8410	3.6093	0.06	0.005	13	13

### 3.3.2 Nonlinear Response Function

An explicit nonlinear function is considered (Yang et al. 2015) as,

$$g(\mathbf{X}) = 2 - \frac{(x_1 - 1)(x_2^2 + 4)}{20} + \sin\left(\frac{5x_2}{2}\right) \quad (3.34)$$

In this example,  $x_1$  and  $x_2$  are p-box uncertain variables with normal distribution. [1.52, 3.48] and [1.4, 1.6] are interval mean values, and 1 and [0.9, 1.1] are the standard deviations of  $x_1$  and  $x_2$  respectively. Since Eq. (3.34) is an explicit function, the IMCS is directly applied to obtain the response bounds with 5,00,000 simulations. Then, first-order HDMR technique is utilised to approximate the responses of the function for  $n = 3, 5, 7$ . Further the function is simulated using the IMCS, and the results are presented in Table 3.3. Figure 3.9 shows the CDF of the response function for different sample points. As the results obtained by the proposed method do not have much variation with respect to the direct IMCS, the deviation of the values is not prominent in Fig. 3.9.

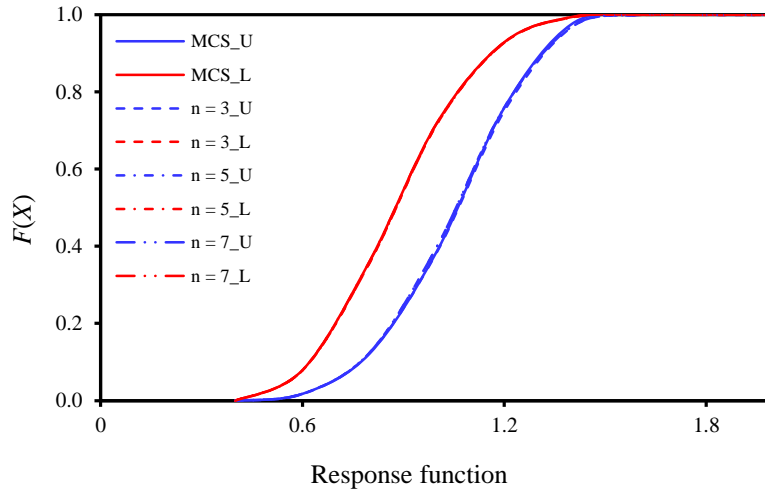


Fig. 3.9 CDF of explicit nonlinear function in Eq. (3.34)



Table 3.3 Response bounds of explicit nonlinear function in Eq. (3.34)

	Response		% Error		Effort	
	LB	UB	LB	UB	LB	UB
Direct IMCS	0.4305	1.4930	-	-	500000	500000
HDMR ( $n=3$ )	0.4420	1.5098	2.67	1.13	5	5
HDMR ( $n=5$ )	0.4407	1.5086	2.37	1.04	9	9
HDMR ( $n=7$ )	0.4400	1.5075	2.21	0.97	13	13

Further, the computational efficiency is studied with respect to number of function evaluations required for estimating the response bounds, as run time of the original complex model reflects the required effort, and the percentage errors observed in the results with reference to the original function are presented in Table 3.3. From the parametric study, for  $n=7$  (from Table 3.3), the error is minimum, and the computational effort is only 13, which is very less compared to the effort required for direct IMCS.

### 3.3.3 Creep-Fatigue Interaction

A nonlinear creep-failure criterion is considered on the basis of creep and fatigue damage accumulation. The initial explicit model is defined as,

$$g(N_c, N_f, n_c, n_f, \theta_1, \theta_2) = 2 - \exp(\theta_1 D_c) + \frac{\exp(\theta_1) - 2}{\exp(\theta_2) - 1} (\exp(-\theta_2 D_c) - 1) - D_f \quad (3.35)$$

Here,  $D_c$  and  $D_f$  are creep damage and fatigue damage by definition,  $D_c = n_c / N_c$  and  $D_f = n_f / N_f$  respectively.  $n_c$  and  $N_c$  are number of loading cycles and life of creep, and  $n_f$  and  $N_f$  are number of loading cycles and life of fatigue.  $\theta_1$  and  $\theta_2$  are experimental parameters. Interval mean and standard deviation of all the p-box variables are listed in Table 3.4.

Table 3.4 Input parameters for creep-fatigue interaction

Variables	Interval Mean	Std. Dev
$N_c$	[5294,5686]	549
$N_f$	[15876,18324]	3420
$n_c$	[496,504]	10
$n_f$	[11737,12263]	600
$\theta_1$	[0.402,0.438]	0.042
$\theta_2$	[5.737,6.263]	0.6

The function in Eq. (3.35) is analysed using the proposed method by deploying three samples along each of the variable axis. The original function was evaluated only at the selected sample point locations, and the corresponding component functions are developed, then the HDMR response function was obtained. The IMCS was applied on the developed HDMR function by simulating the input variables based on their characterization. Bounds of creep are presented in Table 3.5. In this process, 13 number of function evaluations resulted for the construction of the HDMR function. To study the impreciseness of the failure probability, the CDF was drawn for the lower and upper bounds, as shown in Fig. 3.10.

The function was analysed using other available methods like direct IMCS, FORM and SORM. Here, the direct IMCS, which requires 500000 function evaluations, is taken as the reference for the comparison. The proposed technique predicts the failure probability with least computational effort. However, the bounds are wider compared to IMCS. Therefore, the chosen number of sample points along each of the axis was varied from 3 to 7 for seeking improvement in the constructed HDMR model, and the results are presented in Table 3.6 and Fig.3.10.

The CDF for  $n=5$  and  $n=7$  are overlapping exactly with the original function, wherein, the pattern of CDFs for  $n=3$  are significantly showing the deviation, and the curves are wide covering ample of lower and upper bounds.

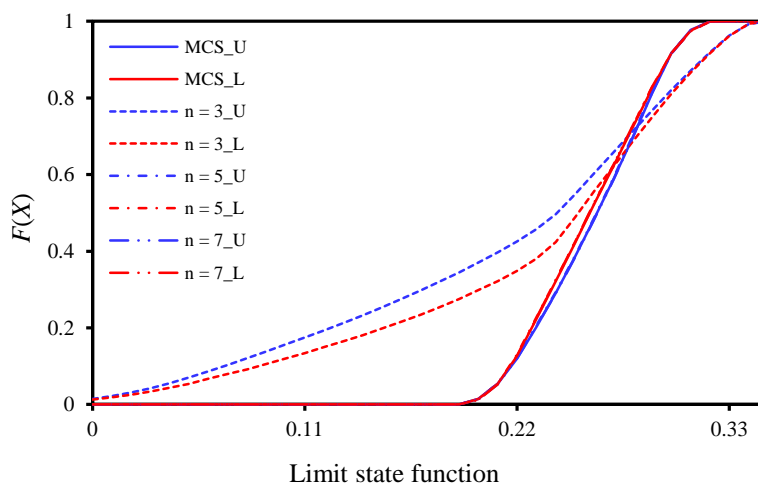


Fig. 3.10 CDF of limit state function for creep-fatigue interaction

Table 3.5 Bounds of creep-fatigue interaction

	Creep		Effort	
	LB	UB	LB	UB
Direct IMCS	0.188	0.322	500000	500000
HDMR ( $n=3$ )	0.131	0.347	13	13
HDMR ( $n=5$ )	0.189	0.324	25	25
HDMR ( $n=7$ )	0.188	0.322	37	37

Table 3.6 Failure probability and reliability index of creep-fatigue interaction

	Failure Probability		Reliability Index		% Error	
	LB	UB	LB	UB	LB	UB
Direct IMCS	0.0032	0.0039	2.6606	2.7266	-	-
HDMR ( $n=3$ )	0.0531	0.0890	1.3469	1.6155	93.97	95.62
HDMR ( $n=5$ )	0.0034	0.0051	2.5690	2.7065	5.88	23.53
HDMR ( $n=7$ )	0.0033	0.0046	2.6045	2.7164	3.03	15.22
FORM	0.0093	0.0156	2.1545	2.3535	65.59	75.00
SORM	0.0178	0.0425	1.7224	2.1015	82.02	90.82

### 3.3.4 Fracture of Turbine Disk

A turbine disk (Jia and Lu 2018) shown in Fig. 3.11 is considered in this example. The radius of crack of the turbine disk exposed to cyclic loading  $N_c$  is defined as,

$$a = \left( \pi^{m/2} (2-m) / 2 \cdot c \cdot N_c (2F\sigma_{\max} / \pi)^m + a_0^{1-m/2} \right)^{2/(2-m)} \quad (3.36)$$

where  $c$ ,  $\sigma_{\max}$  and  $a_0$  represent the crack propagation, maximum stress and the radius of initial crack on the surface of the material. The correction factor ( $F_c$ ), and the crack propagation index ( $m$ ), are taken as 1.122 and 3.285 respectively. The stress intensity factor for maximum stress near crack tip is defined as  $K_{\max} = 2F_c \sqrt{\pi a} / \pi \cdot \sigma_{\max}$ .

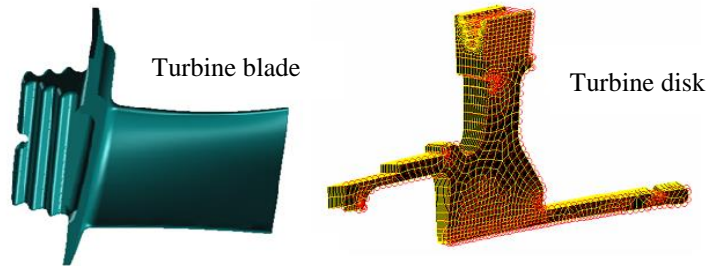


Fig. 3.11 Model of turbine disk

The limit state function is expressed as the difference of critical fracture toughness  $K_{IC}$  and stress intensity factor.

$$g(\sigma_{\max}, K_{IC}) = K_{IC} - 2F_c \sqrt{\pi a} / \pi \cdot \sigma_{\max} - 73 \quad (3.37)$$

The input p-box variables considered for this study are listed in Table 3.7. Practically, the number of loading cycles  $N_c$  can be accurately controlled as a constant, similarly the crack propagation  $c$  as well as the initial surface crack radius  $a_0$  can also be treated as constants when the crack is clear.

Table 3.7 Input parameters for turbine disk

Variables	Interval	Mean	Std. Dev
$\sigma_{\max}$ (MN/m <sup>2</sup> )	[655.7, 694.3]		54.0
$K_{IC}$ (kN/m <sup>1.5</sup> )	[83.9, 90.1]		8.7

The first-order HDMR function is established for the fracture strength of turbine disk by considering  $n$  sample points along each of the variable axes, considering  $\mathbf{c}$  as the mean of p-box variables. Also the function in Eq. (3.37) is evaluated using crude IMCS for comparing the computational effort of the HDMR uncertainty analysis which is appreciably lesser than the original function evaluation. Only five function evaluations were required for obtaining the responses, which is computationally very less intensive compared to the direct IMCS (i.e., 500000 function evaluations). Bounds of fracture strength and failure probability of the function along with reliability index are presented in Tables 3.8 and 3.9 respectively. The corresponding CDFs of the responses are shown in Fig. 3.12.

Table 3.8 Fracture strength of turbine disk

	Fracture Strength (kN/m <sup>1.5</sup> )		Effort	
	LB	UB	LB	UB
Direct IMCS	66.75	73.92	500000	500000
HDMR ( $n=3$ )	66.77	73.93	5	5
HDMR ( $n=5$ )	66.75	73.92	9	9
HDMR ( $n=7$ )	66.75	73.92	13	13

Table 3.9 Failure probability and reliability index of turbine disk

	Failure Probability		Reliability Index		% Error	
	LB	UB	LB	UB	LB	UB
Direct IMCS	0.0172	0.0200	2.0537	2.1154	-	-
HDMR ( $n=3$ )	0.0177	0.0202	2.0496	2.1038	2.82	1.00
HDMR ( $n=5$ )	0.0174	0.0198	2.0579	2.1107	1.14	1.01
HDMR ( $n=7$ )	0.0174	0.0197	2.0579	2.1132	1.14	1.52

Further,  $n$  is varied from 3 to 7 to examine the accuracy. It is evident from Table 3.9 that, the failure probability bounds for the limit state function obtained using HDMR ( $n=3$ ) have a slight variation with reference to the original model. However, for  $n=5$  and 7 the CDFs are exact. The effort taken for getting zero error is (9 evaluations) much lesser than that of the direct IMCS. However, as there is no error resulted for the higher values of  $n$ , the respective bounds are overlapping in Fig. 3.12.

### 3.3.5 Portal Frame Structure

A portal frame structure of single storey and single bay as shown in Fig. 3.13 is considered (Balu and Rao 2013). The cross-sectional areas  $A_1$  and  $A_2$  (log-normal) and horizontal load  $P$  (normal) are modelled as imprecise uncertainties, and their parameters are given in Table 3.10. The values of the second moment of areas are expressed as  $I_i = \alpha_i A_i^2$  ( $i=1,2; \alpha_1 = 0.08333, \alpha_2 = 0.16670$ ).

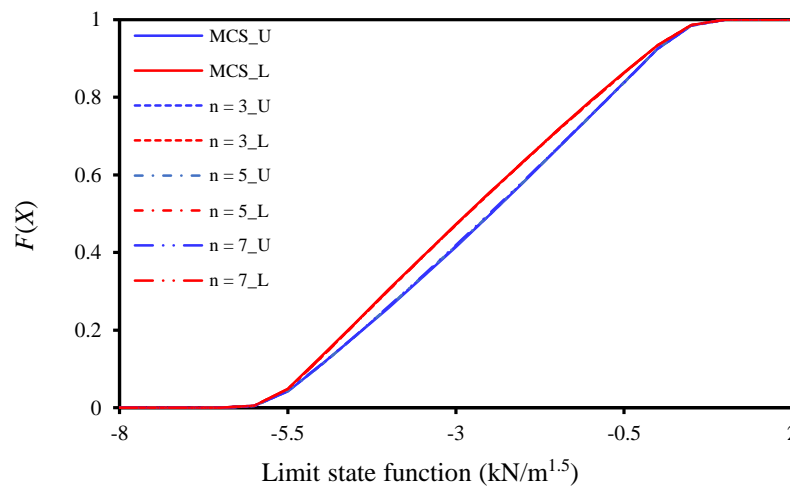


Fig. 3.12 CDF of limit state function for turbine disk

The limit state function is defined for deflection in the horizontal direction at the top of the frame.

$$g(A_1, A_2, P) = \Delta_h - \Delta_{lim} \quad (3.38)$$

where  $\Delta_{lim} = 6 \text{ mm}$  and  $\Delta_h$  is the horizontal displacement.

The limit state function for the displacement of the portal frame is derived using the first-order HDMR technique by distributing  $n$  sample points along each of the variable axis and taking respectively, the mean values of the p-box variables as reference point  $c$ . Bounds of horizontal displacement are presented in Table 3.11.

Table 3.10 Input parameters for portal frame structure

Variables	Distribution	Interval Mean	Std. Dev.
$A_1$ ( $\text{m}^2$ )	Log-normal	[0.325, 0.395]	0.036
$A_2$ ( $\text{m}^2$ )	Log-normal	[0.162, 0.198]	0.018
$P$ (kN)	Normal	[15, 25]	5.0

The failure probability is evaluated for all the values of  $n=3$ . Only seven function evaluations were required for obtaining the responses, which is computationally very less intensive compared to the direct IMCS (i.e., 500000 function evaluations). Bounds of failure probability of the function are presented in Table 3.12, and the corresponding CDFs of the responses are shown in Fig. 3.14. Table 3.12 also presents the bounds of failure probability for sample points  $n=5$  and 7, and FE results by direct IMCS without adopting HDMR for evaluating the efficiency of the methodology. Fig. 3.14 shows CDF of limit state function for different sample points.

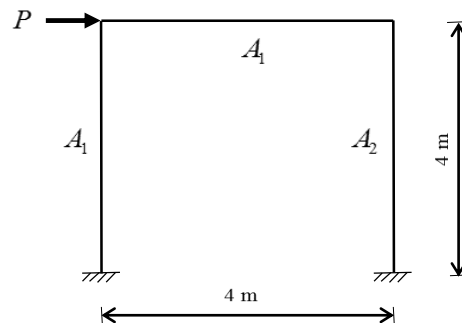


Fig. 3.13 Portal frame structure

Table 3.11 Horizontal displacement of portal frame structure

	Displacement (in mm)		Effort	
	LB	UB	LB	UB
Direct IMCS	2.86	6.89	500000	500000
HDMM ( $n=3$ )	2.63	6.64	7	7
HDMM ( $n=5$ )	2.63	6.66	13	13
HDMM ( $n=7$ )	2.64	6.66	19	19

Table 3.12 Failure probability and reliability index of portal frame structure

	Failure Probability		Reliability Index		% Error	
	LB	UB	LB	UB	LB	UB
Direct IMCS	0.0057	0.0121	2.2539	2.5302	-	-
HDMM ( $n=3$ )	0.0046	0.0082	2.3999	2.6045	23.91	47.56
HDMM ( $n=5$ )	0.0044	0.0082	2.3867	2.6045	29.54	47.56
HDMM ( $n=7$ )	0.0046	0.0085	2.3999	2.6197	23.91	42.35

The results of the frame for three different variables show the different bounds for all sample points when compared with the direct FE analysis using IMCS without adopting HDMM. From Table 3.12, for sample points 3 and 5, bounds are nearer, however  $n=7$  significantly reduces the error with minimum computational effort compared to direct IMCS.

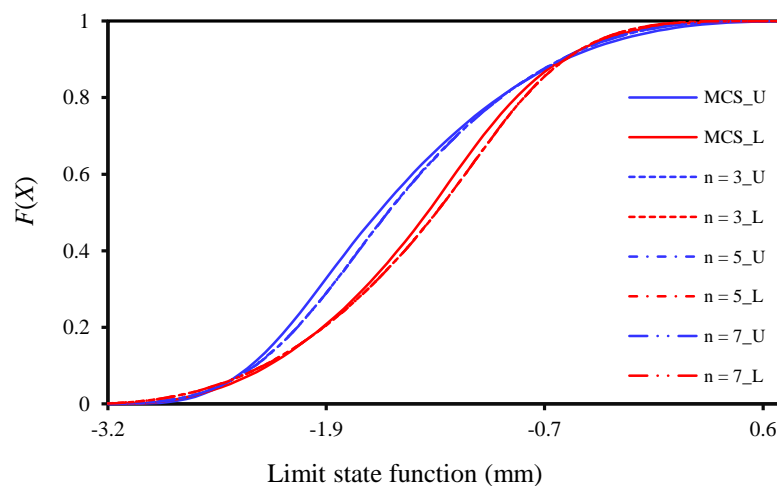


Fig. 3.14 CDF of limit state function for portal frame structure

### 3.3.6 Plane Truss Structure

A 15-bar steel truss structure (Zhang et al. 2010) is studied with small modification, shown in Fig. 3.15. The cross-sectional areas (normal) are  $\mathbf{A} = \{A_1, A_2, \dots, A_{15}\}$  and three loads (log-normal),  $\mathbf{P} = \{P_1, P_2, P_3\}$  are considered as p-box variables for the study. First and second moments are listed in Table 3.13. The limit state function is defined for vertical deflection at the node-5 with limit of 0.06 m.

$$g(A_1, A_2, \dots, A_{15}, P_1, P_2, P_3) = \delta_v - \delta_{\text{lim}} \quad (3.39)$$

where  $\delta_{\text{lim}} = 0.06$  m and  $\delta_v$  is the vertical deflection obtained by the proposed method, and the bounds are presented in Table 3.14. From FE analysis, vertical deflection at node-5 is calculated for all the mean values of variables for deriving the explicit approximated limit state function.

Table 3.13 Input parameters for plane truss structure

Variables	Distribution	Interval Mean	Std. Dev
$A_1$ to $A_6$ ( $\text{m}^2$ )	Normal	[0.001014, 0.001051]	0.00516
$A_7$ to $A_{15}$ ( $\text{m}^2$ )	Normal	[0.000634, 0.000657]	0.00323
$P_1$ (kN)	Log-normal	[84.73, 92.47]	5.836
$P_2$ (kN)	Log-normal	[254.19, 277.44]	15.839
$P_3$ (kN)	Log-normal	[84.73, 92.47]	5.836

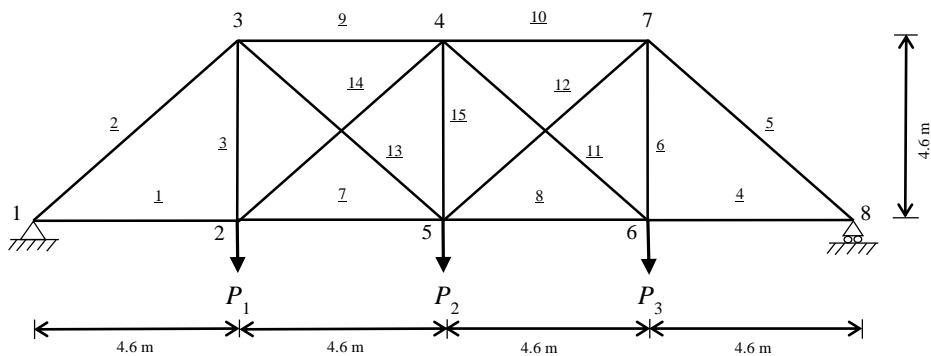


Fig. 3.15 Plane truss structure



Table 3.14 Vertical deflection of plane truss structure

	Deflection (in m)		Effort	
	LB	UB	LB	UB
Direct IMCS	0.0565	0.0624	500000	500000
HDMR ( $n=3$ )	0.0563	0.0623	37	37
HDMR ( $n=5$ )	0.0563	0.0627	73	73
HDMR ( $n=7$ )	0.0566	0.0625	109	109

The failure probability is evaluated for all the values of  $n=3$ . As the number of input variables is high compared to other examples, 37 function evaluations were required for obtaining the responses, which is still computationally very less intensive compared to the direct IMCS (i.e., 500000 function evaluations). Bounds of failure probability and reliability index of the function are presented in Table 3.15, and the corresponding CDFs of the responses are shown in Fig. 3.16.

Table 3.15 Failure probability and reliability index of plane truss structure

	Failure Probability		Reliability Index		% Error	
	LB	UB	LB	UB	LB	UB
Direct IMCS	0.0544	0.1227	1.1616	1.6036	-	-
HDMR ( $n=3$ )	0.0639	0.1068	1.2437	1.5228	14.87	14.89
HDMR ( $n=5$ )	0.0669	0.1113	1.2196	1.4993	18.68	10.24
HDMR ( $n=7$ )	0.0518	0.1247	1.1518	1.6276	5.02	1.60

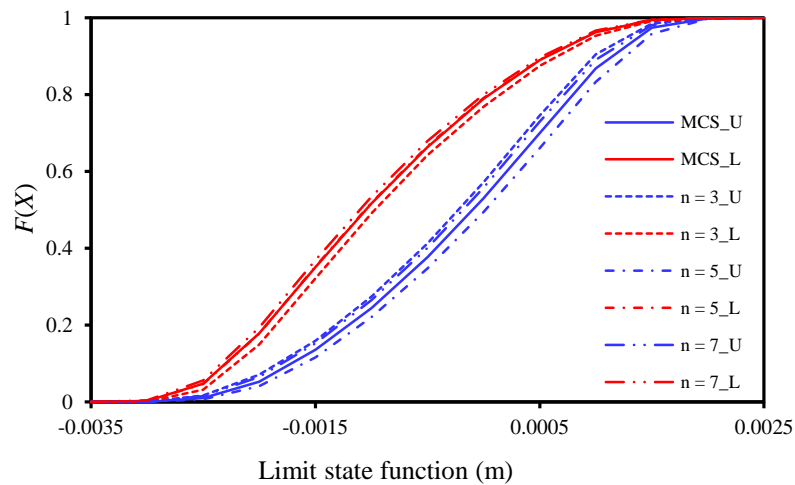


Fig. 3.16 CDF of limit state function for plane truss structure

Similar to the other examples, a parametric study has been carried out for  $n = 3, 5,$  and  $7$ . The errors in the results are compared with that of FE analysis using IMCS. Sample point  $n = 7$  is showing more accurate results compared to  $n = 3$  and  $5$ . The effort taken for FE analysis with IMCS is way greater than the effort taken for sample point  $n = 7$  (i.e., 109).

## CHAPTER 5

### HYBRID STRUCTURAL RELIABILITY

#### 4.1 HYBRID UNCERTAINTIES

Structural reliability estimation gets complicated as number of uncertainties increases, and/or if different sources of uncertainties are present in a system. The hybrid uncertainty analysis merges the diverse types of uncertainty modelling strategies into a single computational scheme. The mixed nature of aleatory and epistemic uncertainties propagated from the model inputs to an output is to be quantified for structural reliability assessment. The performance function with aleatory and epistemic uncertainties can be represented as,

$$g(\mathbf{Z}) = g(\mathbf{X}, \mathbf{Y}) = g(X_1, X_2, \dots, X_r, Y_1, Y_2, \dots, Y_p) \quad (4.1)$$

where  $\mathbf{X} = \{X_1, X_2, \dots, X_r\}$  and  $\mathbf{Y} = \{Y_1, Y_2, \dots, Y_p\}$  are vectors of aleatory and epistemic uncertainties respectively. The uncertainty associated with the model inputs  $\mathbf{X}$  and  $\mathbf{Y}$  are propagated through the model  $g(\mathbf{Z})$ . Balu and Rao (2012b) presented failure probabilities for systems with random and fuzzy variables. Coexistence of random variables and intervals in structural systems was investigated (Bai et al. 2017; Han et al. 2014; Wu et al. 2017) for hybrid reliability approach. Greegar and Manohar (2016) presented global response sensitivity analysis for intervals and fuzzy variables. Zhang et al. (2019) presented a novel approach, chance theory by combining probability theory and uncertainty theory for reliability analysis. Subjective randomness and fuzziness were modelled as uncertainties for the study.

Further, hybrid uncertainties where more than two sources of uncertainties present in the system are taken into account in assessing the structural behaviour. Wang et al. (2014) proposed a hybrid reliability analysis comprising convex theory for structures with multi-source uncertainties. Non-probabilistic boundedness was combined with convex models in different combinations, such as, convex with random, convex with fuzzy random, and convex with interval.

In the present work, vector  $\mathbf{Y}$  is assumed to be divided into sub-vectors as,  $\{Y_1, Y_2, \dots, Y_l\}$ ,  $\{Y_{l+1}, Y_{l+2}, \dots, Y_f\}$  and  $\{Y_{f+1}, Y_{f+2}, \dots, Y_p\}$  representing different sources, intervals, fuzzy and p-box variables respectively as,  $\mathbf{Y} = \{Y_1, Y_2, \dots, Y_l, Y_{l+1}, Y_{l+2}, \dots, Y_f, Y_{f+1}, Y_{f+2}, \dots, Y_p\}$ . Figure 4.1 shows the flowchart for first-order HDMR based hybrid uncertainty analysis. Steps involved in the analysis include, modelling the uncertainties according to the available data by differentiating aleatory and epistemic uncertainties. For the HDMR response surface generation, sample points should be selected on the variable axes and response at each point on the variable axis should be calculated for all the uncertainties. Lagrange's interpolation method is used to interpolate the hidden values on the variable axes to derive the continuous first-order response function. Failure probability bounds are estimated by simulating the response function using IMCS.

## 4.2 RELIABILITY ANALYSIS WITH MIXED UNCERTAINTIES

Nonlinear structural mechanics problems are presented to illustrate the behaviour of structures with mixed variables. First-order HDMR technique is adopted for deriving response function and bounds of system responses, and failure probability are calculated for the same. Sampling is considered from  $n = 3$  to  $7$  where intervals are kept same and sampling is within the bounds.

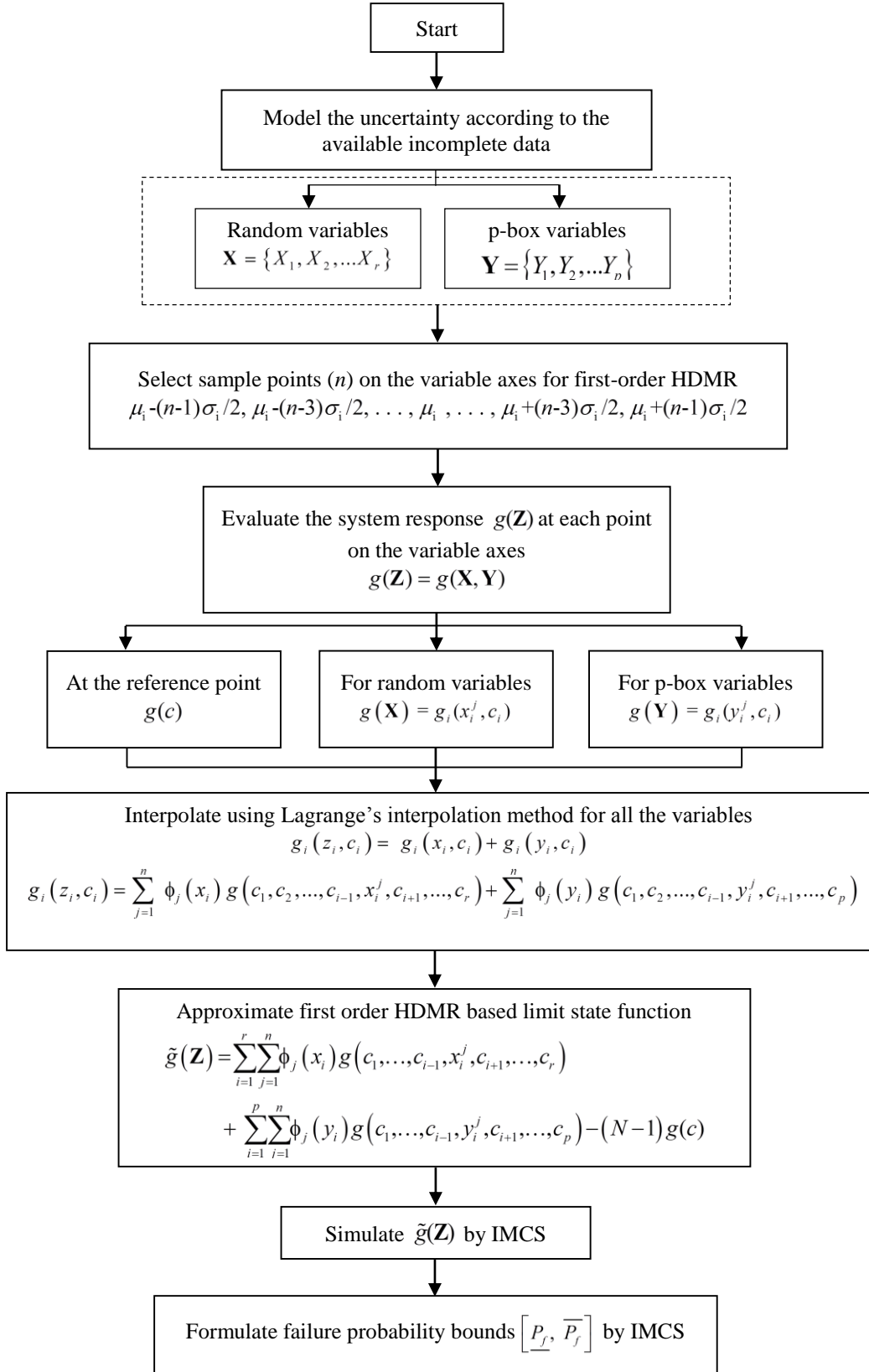


Fig. 4.1 Flowchart for first-order HDMR failure probability for hybrid uncertainties

### 4.2.1 Hollow Cantilever Tube Structure

A cantilever tube is considered as shown in Fig. 4.2 (Jiang et al. 2011).  $F_1, F_2, P$  and  $T$  are the external forces and torsion applied on the cantilever tube respectively. The limit state function is defined for the maximum stress of the cantilever which should be less than the yield strength  $f_y$ , and is expressed as,

$$g(F_1, F_2, P, T, L_1, L_2) = \sigma_{\max} - f_y \quad (4.2)$$

where,  $\sigma_{\max}$  is the maximum von-Mises stress on top surface of the tube, expressed as,

$$\sigma_{\max} = \sqrt{\sigma_x^2 + 3\tau_{zx}^2} \quad (4.3)$$

where  $\sigma_x$  is normal stress. The torsional stress  $\tau_{zx}$ , the area of cross section  $A$ , the bending moment and moment of inertia,  $M$  and  $I$  respectively are expressed as,

$$\sigma_x = \frac{P + F_1 \sin \theta_2 + F_2 \sin \theta_1}{A} + \frac{Md}{2I} \quad (4.4)$$

$$\tau_{zx} = \frac{Td}{4I} \quad (4.5)$$

$$A = \frac{\pi}{4} [d^2 - (d - 2t)^2] \quad (4.6)$$

$$M = F_1 L_1 \cos \theta_2 + F_2 L_2 \cos \theta_1 \quad (4.7)$$

$$I = \frac{\pi}{64} [d^4 - (d - 2t)^4] \quad (4.8)$$

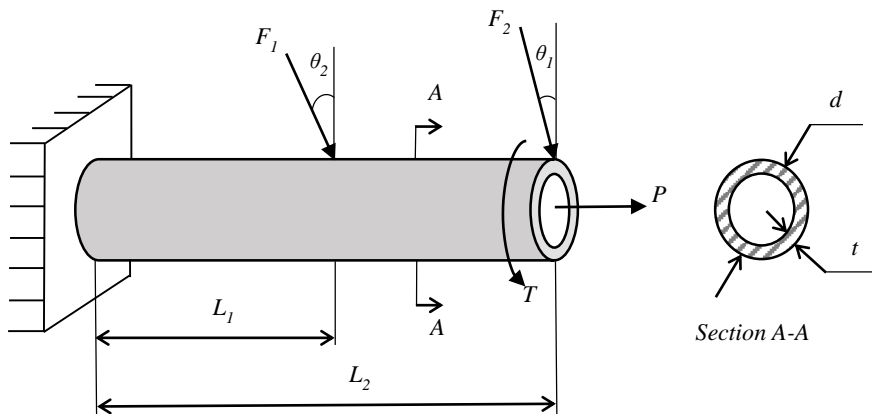


Fig. 4.2 Hollow cantilever tube structure

In this example, the external forces are constructed as p-boxes, and length of the tube is assumed to be normally distributed random variable. The associated distributional parameters are given in Table 4.1. Diameter ( $d$ ) and thickness ( $t$ ) of the tube are considered to be absolute.  $\theta_1$  and  $\theta_2$  are the angles at which  $F_2$  and  $F_1$  are applied to the cantilever tube respectively.

HDMR based mixed uncertainty analysis is carried out for the limit state function in Eq. (4.1), which is a replacement of the explicit expression for maximum von-Mises stress. Also FE analysis is carried out at reference point  $\mathbf{c}$ , for deriving the HDMR approximated limit state function. FE Modelling of the structure is shown in Fig. 4.3, and Table 4.2 presents the  $\sigma_{\max}$  values at all sample points.

Table 4.1 Input mixed uncertainties for hollow cantilever tube structure

Variable	Uncertainty	Distributional parameter-1	Distributional parameter-2
$F_1$ (N)	p-box	[2850, 3150]	300
$F_2$ (N)	p-box	[2850, 3150]	300
$P$ (N)	p-box	[11423, 12638]	[1140, 1260]
$T$ (N-mm)	p-box	[85673, 94782]	[8550, 9450]
$L_1$ (mm)	Random	60	6
$L_2$ (mm)	Random	120	12

The deformed shapes in von-mises and the displacement from FE analysis are shown in Fig. 4.4. Similar to the other examples, a parametric study has been carried out for  $n = 3, 5,$  and  $7$ . The failure probability is evaluated for all the values of  $n$ . As the number of input variables is slightly high, 37 function evaluations were required for obtaining the responses, which is still computationally very less intensive compared to the direct IMCS (i.e., 500000 function evaluations).

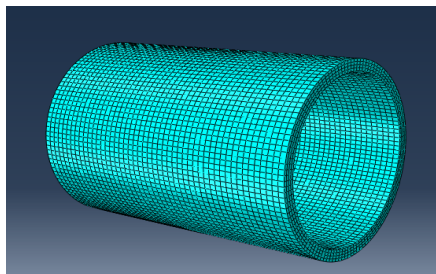


Fig. 4.3 FE model of hollow cantilever tube structure

Table 4.2 Von-Mises stress of hollow cantilever tube structure

	Von-Mises Stress (in MPa)		Effort	
	LB	UB	LB	UB
Direct IMCS	94.03	163.89	500000	500000
HDMR ( $n=3$ )	15.54	175.14	13	13
HDMR ( $n=5$ )	93.22	167.03	25	25
HDMR ( $n=7$ )	94.12	162.92	37	37

Failure probability and corresponding reliability index bounds for HDMR sample points  $n=3$  to  $7$  are presented in Table 4.3 along with the computational efficiency. The error in the values are compared with that of crude IMCS for the explicit function in Eq. (4.3). The corresponding CDFs of limit state function are shown in Fig. 4.5.

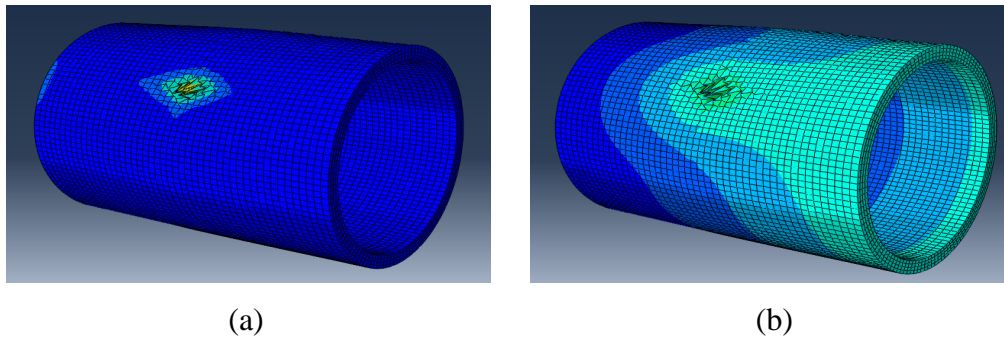


Fig. 4.4 Deformed shape of hollow cantilever tube structure; (a) Mises stress; (b) Displacement

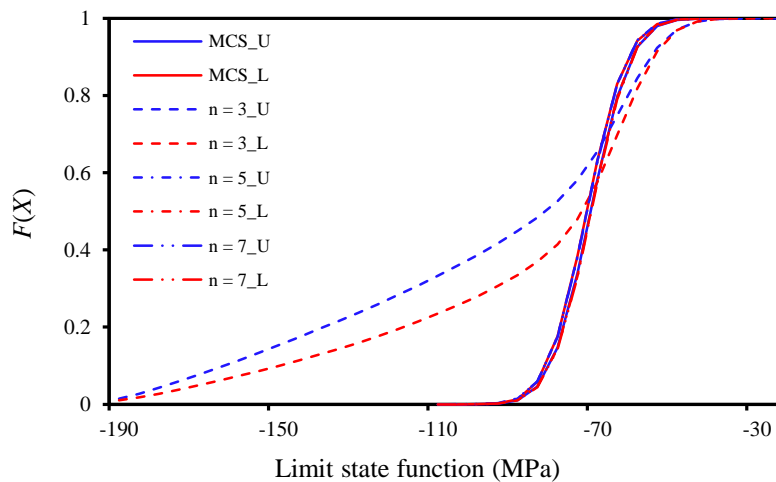


Fig. 4.5 CDF of limit state function for hollow cantilever tube structure



Table 4.3 Failure probability and reliability index of hollow cantilever tube structure

	Failure probability		Reliability Index		% Error	
	LB	UB	LB	UB	LB	UB
Direct IMCS	0.00091	0.0013	3.0224	3.1194	--	--
HDMR ( $n=3$ )	0.01040	0.0095	2.3112	2.3466	91.25	86.32
HDMR ( $n=5$ )	0.00076	0.0011	3.0712	3.1703	16.48	15.38
HDMR ( $n=7$ )	0.00080	0.0011	3.0679	3.1770	12.08	15.38

From Table 4.3, sample point  $n = 7$  is showing more accurate results compared to  $n = 3$  and 5. The effort taken for FE analysis with IMCS is way greater than the effort taken for sample point  $n = 7$  (i.e., 37).

#### 4.2.2 Ten-Storey Irregular RCC structure

Residential and commercial buildings commonly have asymmetric plans and irregularities, which lead to increase in stresses in certain elements and hence result in destruction of the structure. This becomes a concern of safety of the building, if the structure is located in the seismic zone.

Symmetric and asymmetric structures are commonly seen everywhere. In real scenario, most of the structures are asymmetric, due to architectural or aesthetic needs. Asymmetric structures are more vulnerable to earthquakes, hence deformation (or failure) prediction is uncertain when it is compared with symmetric structures.

A ten-storey stiffness irregular reinforced cement concrete (RCC) structures is considered, for the study of behaviour of the structure with irregularity in presence of mixed uncertainties. Since it is an implicit problem, direct simulation is computationally inefficient. Therefore, a regular structure possessing same dimensional and material properties is considered for comparing the results. Figure 4.6 shows plan and elevation of both irregular and regular structures. The dimensions of the structural elements and other data are listed in Table 4.4. The structure is assumed to be located in *zone-V*, with seismic zone factor 0.36. M25 grade of concrete and Fe415 grade of steel are adopted in modelling the structure.

Table 4.4 Input parameters for irregular and regular structures

Variables	Description	Distributional parameter-1	Distributional parameter-2
$E_c$ (MPa)	Modulus of elasticity of concrete	[22.8, 27.2]	5
$b_b$ (mm)	Width of beam	[280, 320]	30
$d_b$ (mm)	Depth of beam	[420, 480]	45
$b_c$ (mm)	Width of column	[280, 320]	30
$d_c$ (mm)	Depth of column	[560, 640]	60
$LL$ (kPa)	Live load	3	0.3

Pushover analysis is carried out for implicit RC structures at reference point for the HDMR sampling as  $g$  (25, 300, 450, 300, 600, 3). The horizontal displacement at the reference point by pushover analysis and linear static analysis at  $n = 3$  and 5 for both the structures are presented in Table 4.5. Hinges formed by pushover analysis for the corresponding displacements are shown in Fig. 4.7. The maximum horizontal displacement for limit state function in Eq. (4.9) for the mixed uncertainties is limited to 500 mm.

$$g(E_c, b_b, d_b, b_c, d_c) = \Delta_h - \Delta_{lim} \quad (4.9)$$

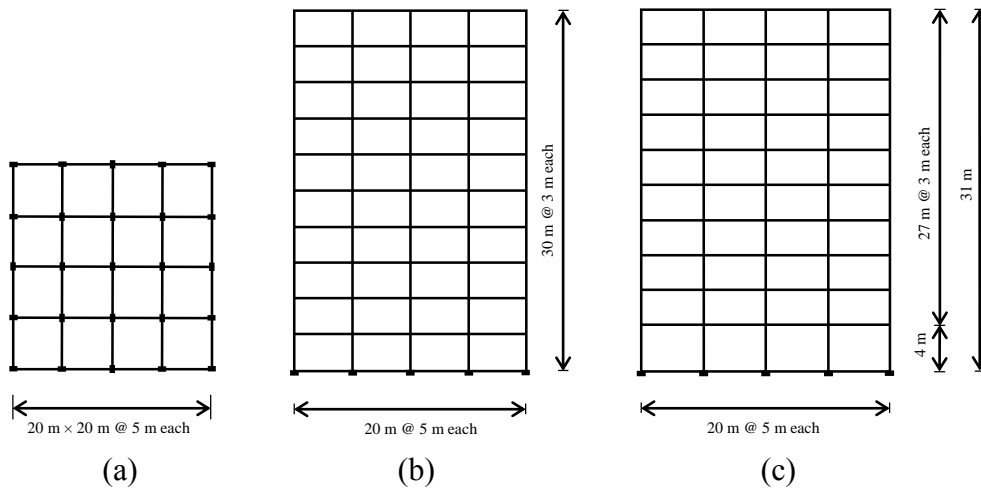


Fig. 4.6 Plan and elevation details; (a) Plan of regular and irregular structures; (b) Elevation of regular structure; (c) Elevation of irregular structure

Table 4.5 Horizontal displacement of irregular and regular structures

	Displacement (in mm)	
	on linear loading	on nonlinear loading
Stiffness irregular RC structure		
at reference point $c$	120	494
HDMR ( $n=3$ )	[36, 171]	[180, 561]
HDMR ( $n=5$ )	[92, 162]	[261, 500]
Regular RC structure		
at reference point $c$	115	486
HDMR ( $n=3$ )	[36, 162]	[160, 540]
HDMR ( $n=5$ )	[85, 152]	[248, 480]

The first-order HDMR function is established for the static linear and static nonlinear (pushover) displacements by considering sample points ( $n = 3$  and  $5$ ) along each of the variable axes, considering  $c$  as the mean values of mixed variables. It is evident from Table 4.5 that, the displacement bounds are getting narrowed from  $n = 3$  to  $5$  for both the structures, wherein, the displacement of stiffness irregular structure is greater to the value of regular structure, in both linear and nonlinear loading.

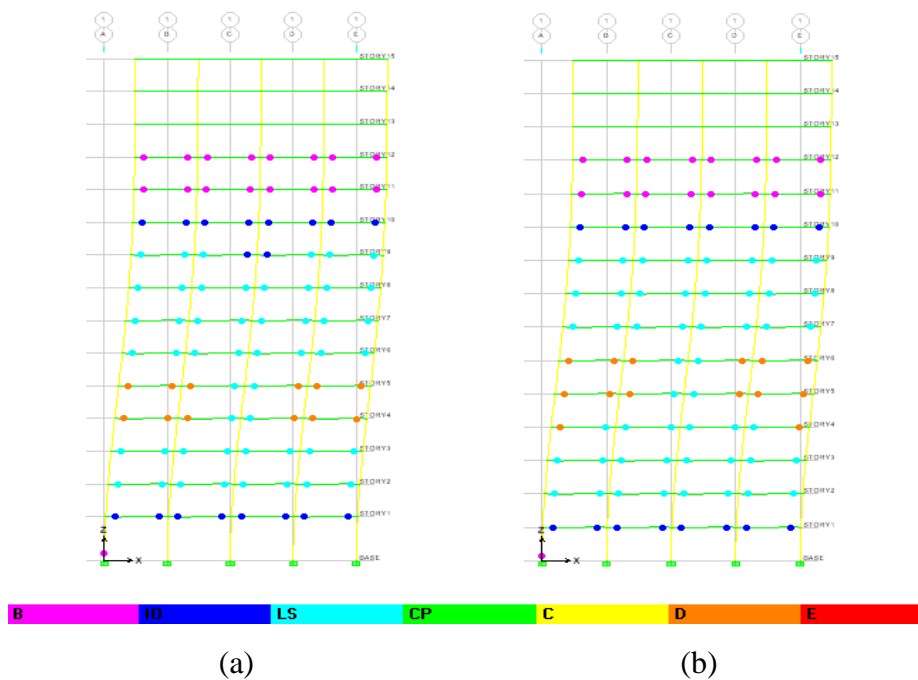


Fig. 4.7 Hinge formation at reference  $c$  for (a) Irregular structure at 10<sup>th</sup> step;  
(b) Regular structure at 12<sup>th</sup> step

25 function evaluations were required for obtaining the responses, which is computationally very less intensive. Bounds of failure probability and reliability index of the function in Eq. (4.9) for nonlinear loading are presented in Table 4.6, and the corresponding CDFs of the limit state function are shown in Figs. 4.8 and 4.9. From the results, it is clear that, the bounds of failure probability of regular structure is wider than the stiffness irregular structure, and the failure probability values for  $n = 5$  are efficient than that of  $n = 3$ , for corresponding displacement values (from Table 4.5).

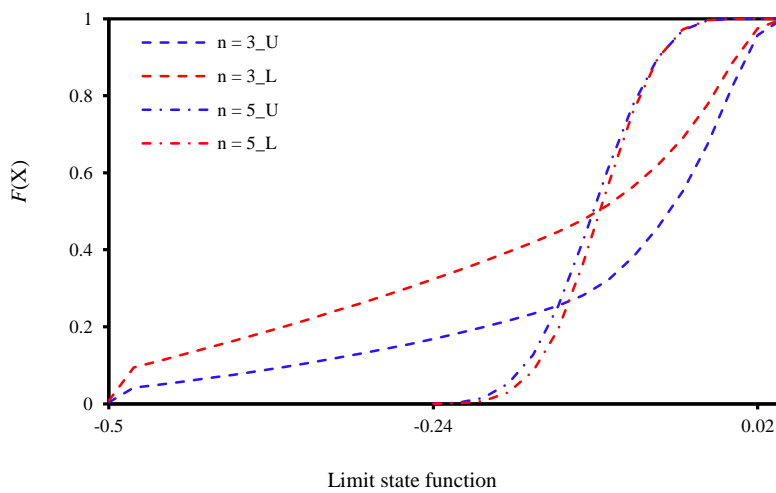


Fig. 4.8 CDF of limit state function for irregular structure

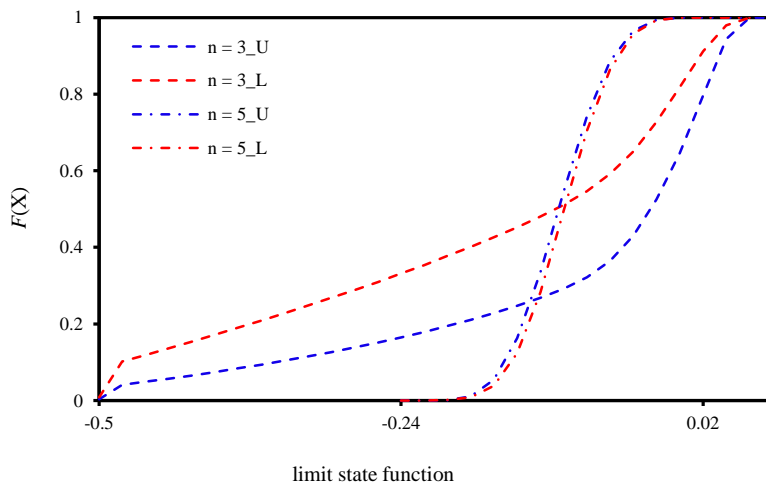


Fig. 4.9 CDF of limit state function for regular structure

Table 4.6 Failure probability and reliability index of irregular and regular structures

	Failure probability		Reliability Index		Effort	
	LB	UB	LB	UB	LB	UB
Stiffness irregular RC structure						
HDMR ( $n=3$ )	0.0110	0.05600	1.2291	1.5897	13	13
HDMR ( $n=5$ )	0.0004	0.00048	3.2990	3.3500	25	25
Regular RC structure						
HDMR ( $n=3$ )	0.03510	0.05380	1.6088	1.8101	13	13
HDMR ( $n=5$ )	0.00016	0.00017	3.5855	3.5921	25	25

### 4.2.3 Nuclear Containment Structure

Nuclear reactor is a device designed to maintain chain reaction producing a steady flow of neutrons generated by the fission of heavy nuclei. Nuclear reactors are used at nuclear power plants for generation of electricity and in propulsion of ships. Heat from nuclear fission is passed to a working fluid (water or gas), which in turn runs through steam turbines. Nuclear reactors are further differentiated either by their purpose or by their design features. In terms of purpose they are either *research reactors* or *power reactors*. Research reactors are operated at universities and research centres. These reactors serve primarily as a neutron source. The neutrons generated are used for multiple purposes such as production of radioisotopes, non-destructive testing, medical research etc. Power reactors are usually found in nuclear power plants. They are dedicated for generating heat mainly for electricity production.

Reactors are designed with the expectation that they will operate safely without releasing radioactivity to their surroundings. It is however recognized that accidents can occur. An approach using multiple fission product barriers has been adopted to deal with such accidents. The containment is the fourth and final barrier to radiation release, the first being the fuel ceramic, the second being the metal fuel claddings, the third being the reactor vessel and coolant system.

The containment structure is a gas-tight shell or other enclosure housing a nuclear reactor to contain the escape of fission products and radioactive gases that otherwise might be released to the atmosphere in the event of an accident. Such

enclosures are usually dome shaped and made of steel reinforced concrete. In practice, the containment structure must be able to maintain its integrity under circumstances of drastic nature. It has to withstand pressure build ups and damage from debris propelled by an energy burst within the reactor, and it must pass appropriate tests to demonstrate that it will not leak more than a small fraction of its contents over a period of several days, even when its internal pressure is well above the surrounding atmospheric pressure. The containment building must also protect components located inside it from external forces such as tsunamis, tornadoes, and airplane crashes.

### ***Containment model***

For this study a 1:4 scaled model has been constructed. It includes all the main features of a prototype such as the pre-stressed concrete cylindrical wall structure with a tori-spherical dome. There are five major openings in the structure, two steam generator openings in the dome along with main air lock, fuelling machine air lock and emergency air lock barrel openings in the cylindrical wall. Figs. 4.10 and 4.11 show cross sectional details of axisymmetric model.

The model includes cylindrical and dome portion along with ring beam and raft. The internal radius of containment model is 6.188m with the cylindrical wall thickness of 188mm and total height of 15.75m. The dome has mean radius of 9.794m and average thickness of 164mm with higher thickness at ring beam and opening locations.

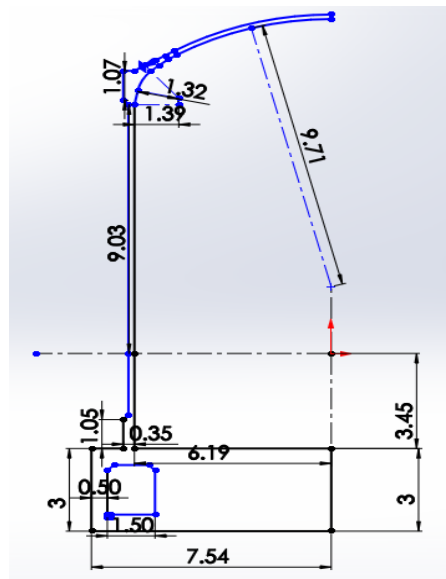


Fig. 4.10 Cross section details of axisymmetric model

The local areas around the openings are thickened to account for the discontinuity effects. The model is pre-stressed by post-tensioning 176 vertical tendons and 108 hoop tendons. A typical vertical tendon is anchored at stressing gallery and ring beam. The hoop tendon is a C-cable which is anchored at buttresses and covers the full circumference of the containment wall. The buttresses are located at 0, 90, 180 & 270 degree. The dome is pre-stressed by 95 J-cables alternately in each direction which continue from raft to the other end of the ring beam. Figures 4.12 and 4.13 show developed view of the hoop and vertical tendons and dome tendons respectively.

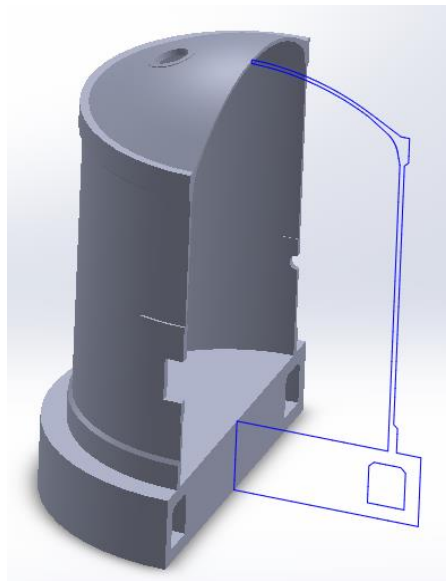


Fig. 4.11 Section view of nuclear containment model

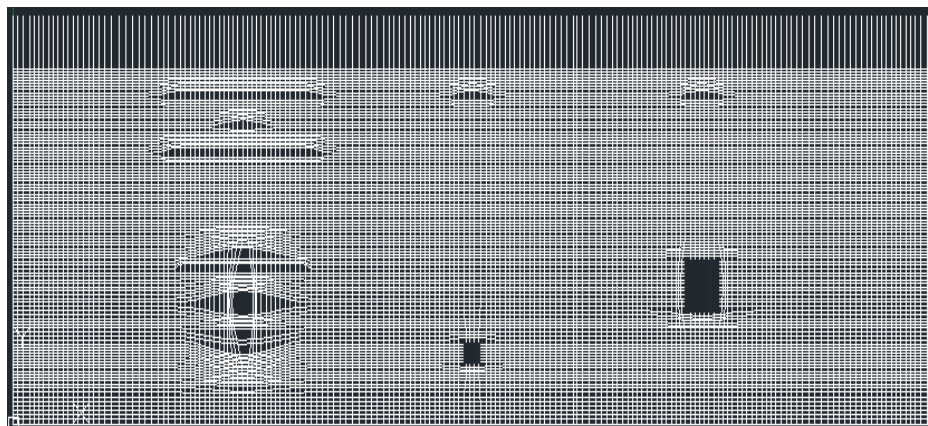
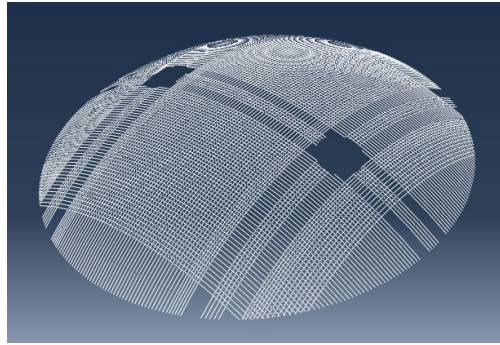


Fig. 4.12 Developed view of the hoop & vertical tendons



(a)



(b)

Fig. 4.13 (a) Dome tendons; and (b) Hoop and vertical tendons

The properties of materials used in the modelling of containment is given in Table 4.7. Concrete damaged plasticity (CDP) model is used for the present study. Model proposed by Hsu and Hsu is used for getting the stress-strain relationship of concrete. Atomic energy regulatory board (AERB) recommends safety codes to ensure nuclear safety in India. One of the recommendations stemming from this requirement is evaluation of ultimate load capacity (ULC) of the containment structure considering pressure load. The objective of this analysis is to understand the behaviour of containment model under internal pressure load and to predict the failure modes with regard to the concrete cracking and tendon inelastic behaviour along with the estimation of ultimate load capacity of the containment model.



Table 4.7 Material properties based on test data

Material	Property	Value
Pre-stressing Tendons	0.2% proof stress (N/mm <sup>2</sup> )	1683
	1% extension stress (N/mm <sup>2</sup> )	1649
	Ultimate tensile strength (N/mm <sup>2</sup> )	1848
	Modulus of elasticity (N/mm <sup>2</sup> )	189600
	Cross-sectional area (mm <sup>2</sup> )	142.8
Concrete	Cube strength ( $f_{ck}$ ) (N/mm <sup>2</sup> )	45
	Modulus of elasticity (N/mm <sup>2</sup> )	33540
	Ultimate tensile strength (N/mm <sup>2</sup> )	2.78

On loading the model in various steps with increase in design pressure  $P_d$ , the ultimate load was attained at  $2.29P_d$ . The model undergoes failure at 0.4% strain in concrete cracking for the ultimate load. Therefore, the model should be designed for the internal pressure load, which should be less than 0.4% strain.

The mixed uncertainties (p-box and random variables) are modelled for the material properties, cross-sectional details, pre-stress and internal pressure loads. The distributional parameters of all the uncertainties are given in Table 4.8. FE analysis has been carried out on the model by considering the structural properties for mean values of all the mixed variables (i.e., at reference point  $c$ ). The limit state function for the containment model is as stated in Eq. (4.10). Figure 4.14 shows FE meshing and deformed shapes of the model.

$$g(E_c, A_t, \sigma_{pt}, P_d) = \varepsilon_{\max} - 0.004 \quad (4.10)$$

In order to study the behaviour of the containment model due to mixed uncertainties, first-order HDMR based uncertainty analysis is carried out. The limit state function for the maximum strain in concrete cracking is derived for sample points  $n = 3$  to  $5$ . The failure probabilities are presented in Table 4.9, along with the computational efficiency. The CDF for the limit state function in Eq. (4.10) are shown in Fig. 4.15.

Table 4.8 Input mixed uncertainties for nuclear containment structure

Variable	Description	Distributional parameter-1	Distributional parameter-2
$E_c$ (MPa)	Modulus of elasticity of concrete	[24524, 31949]	8471
$A_t$ (mm <sup>2</sup> )	Cross-sectional area of tendons	[125, 161]	28.5
$\sigma_{pt}$ (MPa)	Pre-stress load	[869, 1132]	150
$P_d$ (MPa)	Design pressure load	0.144	0.0144

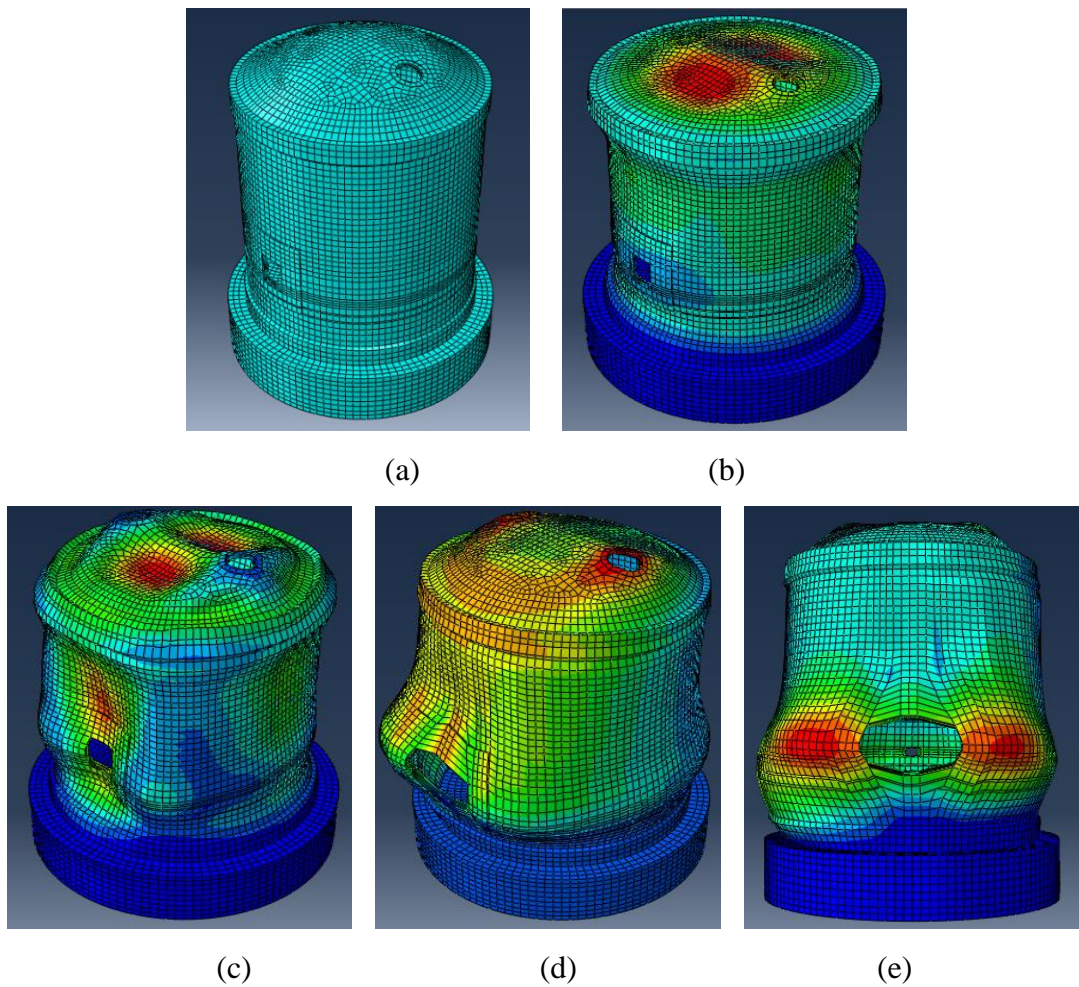


Fig. 4.14 (a) FE meshing of the model; (b) Deformed at self-weight and pre-stressed load; (c) Deformed at design pressure load; (d) Deformed at ULC on dome; and (e) Deformed at ULC on opening

Table 4.9 Failure probability and reliability index of nuclear containment structure

	Failure probability		Reliability Index		Effort	
	LB	UB	LB	UB	LB	UB
HDMR ( $n=3$ )	0.01040	0.0095	2.3112	2.3466	9	9
HDMR ( $n=5$ )	0.00076	0.0011	3.0712	3.1703	17	17

From Fig. 4.15 it is clear that, curves corresponding to sample point  $n = 5$  showing complete deviation from  $n = 3$  on the limit state function for strain values. Bounds are narrowed for  $n = 5$  on the limit state axis.

### 4.3 RELIABILITY ANALYSIS WITH HYBRID UNCERTAINTIES

In order to study the behaviour of systems in presence of various sources of uncertainties, hybrid reliability analysis is carried out using first-order HDMR. Two examples are presented as follows.

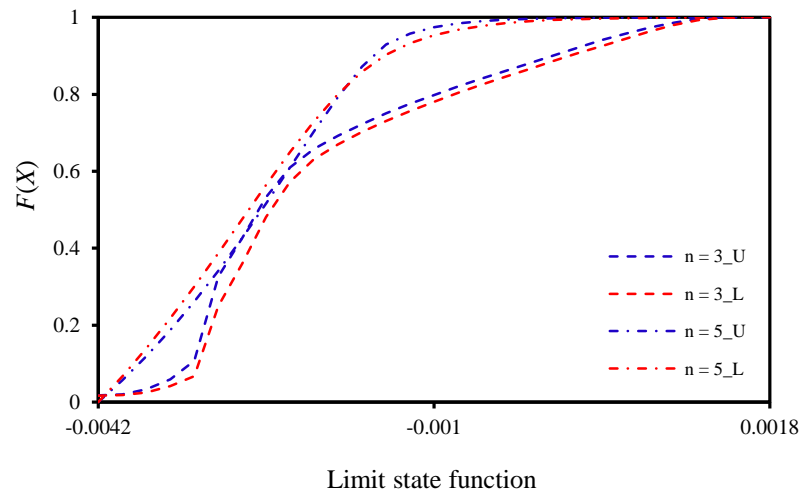


Fig. 4.15 CDF of limit state function for nuclear containment structure

#### 4.3.1 Cantilever Beam Structure

An aluminium cantilever beam shown in Fig. 4.16 is considered for the study of hybrid uncertainties. Combination of a fuzzy variable, an interval, and a random variable along with a p-box variable is taken for the study on the basis of the level of knowledge about the variable. Here, load ( $P$ ) applied at the free end of the beam is assumed to be fuzzy variable with a triangular membership function. Modulus of elasticity ( $E = 69$  GPa)

is considered as deterministic. Details about the uncertainties considered is given in Table 4.10.

Table 4.10 Input hybrid uncertainties for cantilever beam structure

Parameter	Description	Uncertainty	Distributional parameter-1	Distributional parameter-2
$P$ (N)	Load on beam	Fuzzy	[250 275 300]	--
$L$ (mm)	Span of beam	Interval	[760, 770]	--
$b_b$ (mm)	Width of beam	p-box	[24, 26]	3.75
$d_b$ (mm)	Depth of beam	Random	65	13.00

Maximum deflection ( $\delta_{\max}$ ) at the free end is defined explicitly as in Eq. (4.11).

On considering the hybrid uncertainties,  $\delta_{\max}$  is limited to  $\delta_{\lim} = 3$  mm . The limit state function obtained from HDMR based hybrid uncertainty analysis is expressed as in Eq. (4.12).

$$\delta_{\max} = \frac{4PL^3}{Eb_b d_b^3} \quad (4.11)$$

$$g(P, L, b_b, d_b) = \delta_{\max} - \delta_{\lim} \quad (4.12)$$

First-order HDMR hybrid uncertainty analysis is applied for the cantilever beam explicit function bearing hybrid uncertainties. The failure probability curves are shown in Fig. 4.17 for  $n = 3$  to  $7$ . The curve for sample point  $n = 7$  is nearing the values to that of direct MCS which is carried for the function in Eq. (4.11).

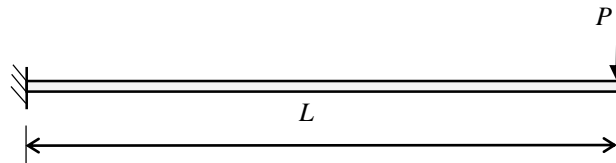


Fig. 4.16 Cantilever beam structure

### 4.3.2 Plane Truss Structure

A 15-bar steel truss structure (Zhang et al. 2010) is considered as shown in Fig. 3.15. In this example, the cross-sectional areas and three loads (at node-2, 5 and 6), are modelled as the p-boxes, interval, fuzzy and random uncertainties respectively

considered for the HDMR based hybrid uncertainty analysis. Input hybrid uncertainties are given in Table 12 along with the corresponding distributional parameters. The limit state function is defined for vertical deflection at the node-5 limited to  $\delta_{lim} = 0.06$  m .

$$g(A_1, A_2, \dots, A_{15}, P_1, P_2, P_3) = \delta_v - \delta_{lim} \quad (4.13)$$

From FE analysis, vertical deflection at node-5 is calculated for all the mean values of variables for deriving the explicit approximated limit state function. The failure probability is evaluated for all the values of  $n=3$  to  $7$ . As the hybrid uncertainties varies characteristically, the failure probabilities obtained resulted in wide trapezoidal membership curves, as shown in Fig 4.18.

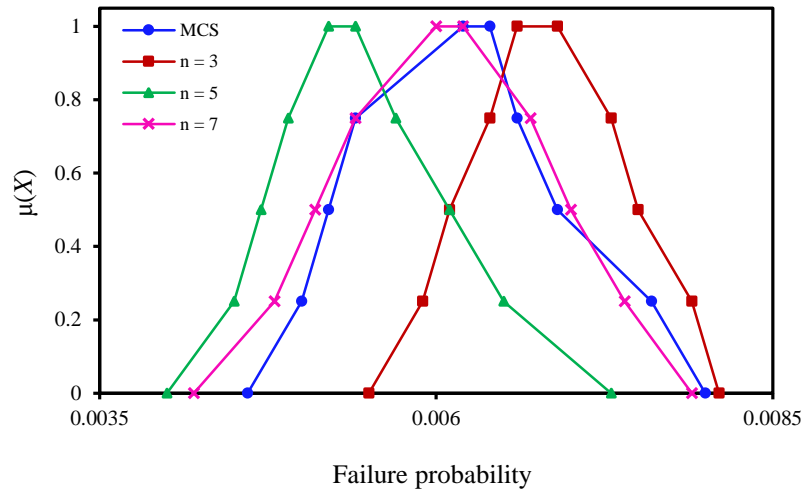


Fig. 4.17 Failure probability curves of cantilever beam structure

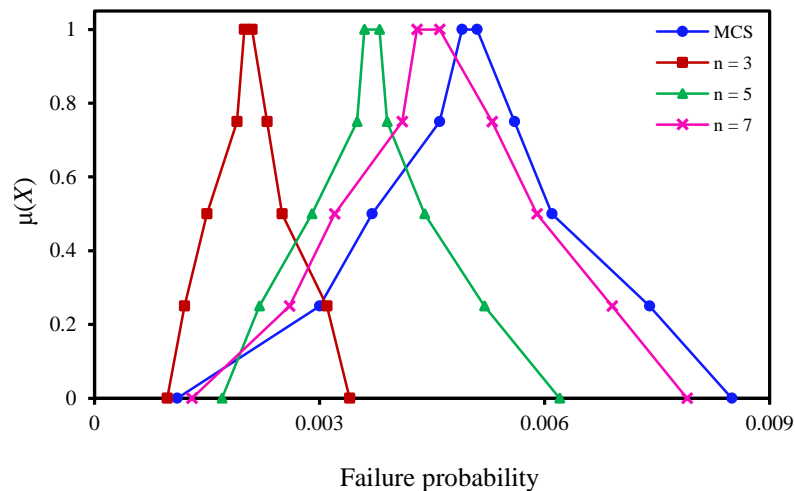


Fig. 4.18 Failure probability curves of plane truss structure with hybrid uncertainties

Table 12 Input hybrid uncertainties for plane truss structure

Variables	Uncertainty	Distributional parameter-1	Distributional parameter-2
$A_1$ to $A_6$ ( $m^2$ )	p-box	[0.001014, 0.001051]	0.0000516
$A_7$ to $A_{15}$ ( $m^2$ )	p-box	[0.000634, 0.000657]	0.0000323
$P_1$ (kN)	Interval	[85, 95]	--
$P_2$ (kN)	Fuzzy	[250 275 300]	--
$P_3$ (kN)	Random	90	18

As the number of variables is high compared to other examples, 109 function evaluations were required for obtaining the responses for  $n=7$  which is still computationally very less intensive compared to the direct IMCS (i.e., 500000 function evaluations). From Fig. 4.18, sample point  $n=7$  is showing more accurate results as compared to  $n=3$  and 5.

## CHAPTER 5

### SUMMARY AND CONCLUSION

#### 5.1 RESULTS AND DISCUSSIONS

Uncertainty is inherent in most of the physical processes, and it should be quantified efficiently so as to make the design more reliable and optimum. Primarily, appropriate characterization of uncertain input is essential, however, it is a challenging task while dealing with the limited information. Moreover, in real-time systems, it is sensible to consider different kinds of uncertainties in the system, when the information of the uncertainties have impreciseness and originate from different sources.

In this context, a computationally efficient uncertainty analysis procedure is presented in this study to estimate the failure probability of structural systems by modelling the imprecise input as probability-box. The numerical examples possessing the explicit relationships are directly used in simulation, and also the function is approximated using first-order HDMR, in which the polynomial type function replaces the original nonlinear function for studying the efficiency of the HDMR in imprecise uncertain situations. The number of sample points in each of the variable axis is varied from 3 to 7 so that the improvement in the accuracy of the approximated HDMR function is witnessed.

In all the numerical examples, the bounds of failure probabilities obtained from the proposed method are closer to the bounds of original models evaluated by crude Monte Carlo method. Also the results are obtained with lesser effort and more efficiently. In the example of creep-fatigue interaction, it is evident that sample point  $n = 5$  is showing accuracy for failure probability bounds with the direct IMCS results with lesser error of 5.88% for LB and 23.53% for UB. Further, the sample point  $n = 7$  is showing even lesser error of 3.03% and 15.22% for LB and UB respectively, which is acceptably lesser than the results obtained from conventional methods i.e., FORM and SORM. As these methods are approximation methods, the explicit function is going to carry a considerable amount of error in the results. Further if the HDMR based limit state function is simulated by these methods, the accumulated error will give huge

deviation from the original model. It can be witnessed from Table 3.6 that, FORM and SORM results on the model are showing acute amount of error as [65.59%, 75%] and [82.02%, 90.82%] respectively, whereas in case of fracture turbine disk example,  $n = 7$  shows the lesser percentage of error [1.14%, 1.52%] with the lesser effort of 13 evaluations compared to direct IMCS (i.e., 500000 evaluations).

In the case of implicit situations, the FE analysis of real complex models requires tremendous effort for simulating the model many times, which is computationally tedious. Therefore, first-order HDMR is adopted to derive the explicit limit state function before the simulation is performed. In the example of portal frame structure,  $n = 5$  shows nearer bounds of failure probability, i.e., [0.0044, 0.0088], but further  $n = 7$  has no much improvement in the results of failure probability bounds [0.0046, 0.0085]. Though plane truss structure example requires more effort compared to other examples (109 evaluations for  $n = 7$ ) with eighteen number of p-boxes that is lesser to the direct IMCS (for 500000 function evaluations). The structure exhibits similar trend of results, where  $n = 7$  has lesser error of [5.02%, 1.60%] with respect to failure probability bounds obtained from direct IMCS.

An attempt has been made to study the behaviour of structural systems, when more than two sources of uncertainties are present. In hollow cantilever tube example, lesser error in the failure probability bounds of [0.0008, 0.0011] for  $n = 7$  is observed as compared to the original model evaluation from the IMCS with high efficiency in presence of mixed uncertainties, where probability-box and random variables coexist in the system simultaneously.

Real-time examples have been considered for validating the proposed methodology. The mixed uncertainties present in both the systems are modelled as probability-box and random variables with corresponding distributional parameters. As the systems are of multi-dimension, the run time of model is too high, specially for nuclear containment example. The model takes 5-days for a single run in ABAQUS finite element package on a computer (with 8GB RAM). Hence sample points of 3 and 5 have been considered for deriving HDMR limit state function.

Nuclear containment structure is an implicit nonlinear example, which has been modelled for mixed uncertainties. The failure probability bounds are tight for  $n = 5$  as



compared to  $n = 3$  for the limit state function derived from HDMR. The effort taken for deriving HDMR function is 17 number of evaluations. In the irregular RC structure example, failure probability bounds are getting narrowed from  $n = 3$  to  $n = 5$ . Also, the results are compared with a regular RC structure possessing same structural parameters. And observed similar trend in the failure probability bounds.

Cantilever beam and plane truss structures are considered in the present work, in order to study the behaviour of model accommodating hybrid uncertainties comprising random, interval and fuzzy variables along with p-box. Since there exist interval variable with lower and upper bounds, and fuzzy variable with triangular membership function, the resulting failure probability is a trapezoidal membership function. For both the examples, failure probability curves for  $n = 7$  are nearer to the original model.

## 5.2 CONCLUSIONS

The simulation of the original explicit nonlinear function over million times is evidently cumbersome. Moreover, in case of implicit situations, the FE analysis carried out for original function evaluation with IMCS is very tedious, as each run takes more time. Therefore, first-order HDMR is adopted to derive the limit state function, and the simulation is performed on the HDMR function. The CDFs are presented for all the bounds of the limit state function, as the input variables are represented by imprecise probability distributions. Distributions of all the variables are predefined and no assumptions are introduced in the numerical examples. The proposed method holds good for all kinds of distributions of parameters with inadequate statistical data.

From the results obtained using the proposed methodology, the application of HDMR makes the uncertainty quantification more efficient when the imprecise uncertainties are characterised as p-box variables in the systems. It is recommended that the proposed method can be applied to any kind of imprecise uncertainties with less computational effort without compromising on the accuracy.

## **5.2 SCOPE FOR FUTURE WORK**

- i. In the present work, first order HDMR expansions are utilized to develop the response equations. The accuracy can be significantly improved by employing the second order HDMR, but with slightly increased computational effort.
- ii. Time variant reliability problems with imprecise uncertainties can be solved in time-dependent situations.
- iii. Inverse reliability assessment can be done by utilizing optimization techniques considering the imprecise uncertainties.

## REFERENCES

- [1] Alyanak, E., Grandhi, R. and Bae, H. (2008). “Gradient projection for reliability-based design optimization using evidence theory.” *Engineering Optimization*, 40(10), 923–935.
- [2] Astroza, R., Ebrahimian, H., Li, Y. and Conte, J.P. (2017). “Bayesian nonlinear structural FE model and seismic input identification for damage assessment of civil structures.” *Mechanical Systems and Signal Processing*, 93, 661–687.
- [3] Bai, B., Zhang, W., Li, B., Li, C. and Bai, G. (2017). “Application of probabilistic and non-probabilistic hybrid reliability analysis based on dynamic sub-structural extremum response surface decoupling method for a blisk of the aeroengine.” *International Journal of Aerospace Engineering*, Hindwai Article ID–5839620, pages 1–11.
- [4] Balesdent, M., Brevault, L., Lacaze, S., Missoum, S. and Morio, J. (2016). “Methods for high-dimensional and computationally intensive models.” In *Estimation of Rare Event Probabilities in Complex Aerospace and Other Systems: A Practical Approach*, 109–136.
- [5] Balu, A.S. and Rao, B.N. (2011). “Efficient explicit formulation for practical fuzzy structural analysis.” *Sadhana - Academy Proceedings in Engineering Sciences*.
- [6] Balu, A.S. and Rao, B.N. (2012a). “High dimensional model representation based formulations for fuzzy finite element analysis of structures.” *Finite Elements in Analysis and Design*, 50, 217–230.
- [7] Balu, A.S. and Rao, B.N. (2012b). “Inverse structural reliability analysis under mixed uncertainties using high dimensional model representation and fast Fourier transform.” *Engineering Structures*, 37, 224–234.
- [8] Balu, A.S. and Rao, B.N. (2013). “Confidence bounds on design variables using high-dimensional model representation-based inverse reliability analysis.” *Journal of Structural Engineering*, 139(6), 985–996.
- [9] Balu, A.S. and Rao, B.N. (2014). “Efficient assessment of structural reliability in presence of random and fuzzy uncertainties.” *ASME Journal of Mechanical Design*, 136(5), 051008.

- [10] Becker, W., Oakley, J.E., Surace, C., Gili, P., Rowson, J. and Worden, K. (2012). “Bayesian sensitivity analysis of a nonlinear finite element model.” *Mechanical Systems and Signal Processing*, 32, 18–31.
- [11] Beer, M., Ferson, S. and Kreinovich, V. (2013). “Imprecise probabilities in engineering analyses.” *Mechanical Systems and Signal Processing*, 37(1–2), 4–29.
- [12] Ben-Haim, Y. and Elishakoff, I. (1990). *Convex models of uncertainty in applied mechanics*. Netherlands, Elsevier.
- [13] Biswal, S. and Ramaswamy, A. (2017). “Finite element model updating of concrete structures based on imprecise probability.” *Mechanical Systems and Signal Processing*, 94, 165–179.
- [14] Bucher, C. and Most, T. (2008). “A comparison of approximate response functions in structural reliability analysis.” *Probabilistic Engineering Mechanics*, 23(2-3), 154-163.
- [15] Chakraborty, S., Chatterjee, T., Chowdhury, R. and Adhikari, S. (2017). “A surrogate based multi-fidelity approach for robust design optimization.” *Applied Mathematical Modelling*, 47, 726–744.
- [16] Choi, S.K., Grandhi, R.V. and Canfield, R.A. (2007). *Reliability-based Structural Design*. Springer Science and Business Media.
- [17] Chowdhury, R., Rao, B.N. and Prasad, A.M. (2008). “High dimensional model representation for piece-wise continuous function approximation.” *Communications in Numerical Methods in Engineering*, 24, 1587–1609.
- [18] Chowdhury, R., Rao, B. N., and Prasad, A. M. (2009). “Stochastic sensitivity analysis using HDMR and score function.” *Sadhana*, 34, 967–986.
- [19] Crespo, L.G., Kenny, S.P. and Giesy, D.P. (2013). “Reliability analysis of polynomial systems subject to p-box uncertainties.” *Mechanical Systems and Signal Processing*, 37(1–2), 121–36.
- [20] Czarnecki, A.A. and Nowak, A.S. (2008). “Time-variant reliability profiles for steel girder bridges.” *Structural Safety*, 30(1), 49–64.
- [21] Dey, S., Mukhopadhyay, T., Sahu, S.K. and Adhikari, S. (2016). “Effect of cutout on stochastic natural frequency of composite curved panels.” *Composites Part B: Engineering*, 105, 188–202.

- [22] Dey, S., Mukhopadhyay, T., Sahu, S.K. and Adhikari, S. (2018). “Stochastic dynamic stability analysis of composite curved panels subjected to non-uniform partial edge loading.” *European Journal of Mechanics-A/Solids*, 67, 108–122.
- [23] Ditlevsen, O. and Madsen, H.O. (1996). *Structural Reliability Methods*. John Wiley and Sons Ltd, New York.
- [24] Dolšek, M. (2012). “Simplified method for seismic risk assessment of buildings with consideration of aleatory and epistemic uncertainty.” *Structure and Infrastructure Engineering*, 8(10), 939–953.
- [25] Du, X. (2008). “Saddlepoint approximation for sequential optimization and reliability analysis.” *ASME Journal of Mechanical Design*, 130, 011011.
- [26] Echard, B., Gayton, N., Lemaire, M. and Relun, N. (2013). “A combined importance sampling and kriging reliability method for small failure probabilities with time-demanding numerical models.” *Reliability Engineering and System Safety*, 111, 232–240.
- [27] Faes, M. and Moens, D. (2019). “Recent trends in the modeling and quantification of non-probabilistic uncertainty.” *Archives of Computational Methods in Engineering*, 1–39.
- [28] Faravelli, L. (1989). “Response surface approach for reliability analysis.” *Journal of Engineering Mechanics*, 115(12), 2763–2781.
- [29] Feng, T., Zhang, S. and Mi, J. (2012). “The reduction and fusion of fuzzy covering systems based on the evidence theory.” *International Journal of Approximate Reasoning*, 53(1), 87–103.
- [30] Ferson, S., Kreinovich, V., Ginzburg, L., Myers, D. and Sentz, K. (2002). “Constructing probability boxes and Dempster-Shafer structures.” *Technical report*, SANDD202–4015.
- [31] Gao, W., Wu, D., Gao, K., Chen, X. and Tin-Loi, F. (2018). “Structural reliability analysis with imprecise random and interval fields.” *Applied Mathematical Modelling*, 55, 49–67.
- [32] Giunta, A.A., McFarland, J.M., Swiler, L.P. and Eldred, M.S. (2006). “The promise and peril of uncertainty quantification using response surface approximations.” *Structures and Infrastructure Engineering*, 2(3–4), 175–189.

- [33] Greegar, G. and Manohar, C.S. (2016). “Global response sensitivity analysis of uncertain structures.” *Structural Safety*, 58, 94–104.
- [34] Guimarães, H., Matos, J.C. and Henriques, A.A. (2018). “An innovative adaptive sparse response surface method for structural reliability analysis.” *Structural Safety*, 73, 12–28.
- [35] Guo, S.X. and Lu, Z.Z. (2015). “A non-probabilistic robust reliability method for analysis and design optimization of structures with uncertain-but-bounded parameters.” *Applied Mathematical Modelling*, 39(7), 1985–2002.
- [36] Hajikolaie, K.H. and Wang, G.G. (2014). “High Dimensional model representation with principal component analysis.” *ASME Journal of Mechanical Design*, 136(1), 1–11.
- [37] Han, X., Jiang, C., Liu, L., Liu, J. and Long, X. (2014). “Response surface based structural reliability analysis with random and interval mixed uncertainties.” *Science China Technological Sciences*, 57(7), 1322–1334.
- [38] Hawchar, L. and Soueidy, C.E. (2015). “Time-variant reliability analysis using polynomial chaos expansion.” In *Proceeding of International Conference on Applications of Statistics and Probability in Civil Engineering*, Vancouver, Canada, 1–7.
- [39] He, Y., Mirzargar, M. and Kirby, R.M. (2015). “Mixed aleatory and epistemic uncertainty quantification using fuzzy set theory.” *International Journal of Approximate Reasoning*, 66, 1–15.
- [40] Hou, Y.H., Li, Y.J. and Liang, X. (2019). “Mixed aleatory/epistemic uncertainty analysis and optimization for minimum EEDI hull form design.” *Ocean Engineering*, 172, 308–315.
- [41] Hu, Z. and Mahadevan, S. (2017). “Adaptive surrogate modeling for time-dependent multidisciplinary reliability analysis.” *ASME Journal of Mechanical Design*, 140(2), 021401.
- [42] Jha, B.N. and Li, H.S. (2017). “Structural reliability analysis using a hybrid HDMR-ANN method.” *Journal of Central South University*, 24(11), 2532–2541.

- [43] Jia, B. and Lu, Z. (2018). “Root finding method of failure credibility for fuzzy safety analysis.” *Structural and Multidisciplinary Optimization*, 58(5), 1917–1934.
- [44] Jiang, C., Li, W.X., Han, X., Liu, L.X. and Le, P.H. (2011). “Structural reliability analysis based on random distributions with interval parameters.” *Computers and Structures*, 89, 2292–2302.
- [45] Jiang, C., Lu, G.Y., Han, X. and Liu, L.X. (2012). “A new reliability analysis method for uncertain structures with random and interval variables.” *International Journal of Mechanics and Materials in Design*, 8(2), 169–182.
- [46] Jiang, L. and Li, X. (2015). “Multi-element least square HDMR methods and their applications for stochastic multiscale model reduction.” *Journal of Computational Physics*, 294, 439–461.
- [47] Jiang, T., Chen, J.J. and Xu, Y.L. (2007). “A semi-analytic method for calculating non-probabilistic reliability index based on interval models.” *Applied Mathematical Modelling*, 31, 1362–1370.
- [48] Karanki, D.R., Kushwaha, H.S., Verma, A.K. and Ajit, S. (2009). “Uncertainty analysis based on probability bounds (p-box) approach in probabilistic safety assessment.” *Risk Analysis*, 29(5), 662–675.
- [49] Kaya, H., Kaplan, M. and Saygın, H. (2004). “A recursive algorithm for finding HDMR terms for sensitivity analysis.” *Computer Physics Communications*, 158, 106–112.
- [50] Kim, S. and Na, S. (1997). “Response surface method using vector projected sampling points.” *Structural Safety*, 19(1), 3–19.
- [51] Lambert, R.S.C., Lemke, F., Kucherenko, S.S., Song, S. and Shah, N. (2016). “Global sensitivity analysis using sparse high dimensional model representations generated by the group method of data handling.” *Mathematics and Computers in Simulation*, 128, 42–54.
- [52] Lee, I., Choi, K.K., Noh, Y., Zhao, L. and Gorsich, D. (2011). “Sampling-based stochastic sensitivity analysis using functions for RBDO problems with correlated random variables.” *ASME Journal of Mechanical Design*, 133(2), 021003.

- [53] Li, E., Ye, F. and Wang, H. (2017a). “Alternative Kriging-HDMR optimization method with expected improvement sampling strategy.” *Engineering Computations*, 34(6), 1807–1828.
- [54] Li, G., Lu, Z., Li, L. and Ren, B. (2016). “Aleatory and epistemic uncertainties analysis based on non-probabilistic reliability and its kriging solution.” *Applied Mathematical Modelling*, 40, 5703–5716.
- [55] Li, G., Wang S.W. and Rabitz, H. (2000). “High dimensional model representations (HDMR): Concepts and applications.” In *Proceedings of the Institute of Mathematics and Its Applications Workshop on Atmospheric Modeling*, Citeseer, 15–19.
- [56] Li, G., Xing, X., Welsh, W. and Rabitz, H. (2017b). “High dimensional model representation constructed by support vector regression. I. Independent variables with known probability distributions.” *Journal of Mathematical Chemistry*, 55(1), 278–303.
- [57] Li, H. and Foschi, R.O. (1998). “An inverse reliability method and its application.” *Structural Safety*, 20, 257–270.
- [58] Liu, X. and Zhang, Z. (2014). “A hybrid reliability approach for structure optimisation based on probability and ellipsoidal convex models.” *Journal of Engineering Design*, 25(4–6), 238–258.
- [59] Liu, X., Kuang, Z., Yin, L. and Hu, L. (2017). “Structural reliability analysis based on probability and probability box hybrid model.” *Structural Safety*, 68, 73–84.
- [60] Liu, Y., Jeong, H.K. and Collette, M. (2016). “Efficient optimization of reliability-constrained structural design problems including interval uncertainty.” *Computers and Structures*, 177, 1–11.
- [61] Lü, H., Shangguan, W. and Yu, D. (2016). “Squeal reduction of a disc brake system with fuzzy uncertainties.” *Journal of Vibroengineering*, 18(6), 3981–4001.
- [62] Luo, Y., Kang, Z. and Li, A. (2009). “Structural reliability assessment based on probability and convex set mixed model.” *Computers and Structures*, 87, 1408–1415.



- [63] Mejri, M., Cazuguel, M. and Cognard, J.Y. (2011). “A time-variant reliability approach for ageing marine structures with non-linear behaviour.” *Computers and Structures*, 89(19–20), 1743–1753.
- [64] Melchers, R.E. (2003). “Probabilistic model for marine corrosion of steel for structural reliability assessment.” *ASCE Journal of Structural Engineering*, 129(11), 1484–1493.
- [65] Moens, D. and Vandepitte, D. (2004). “A survey of non-probabilistic uncertainty treatment in finite element analysis.” *Computer Methods in Applied Mechanics and Engineering*, 194(12–16), 1527–1555.
- [66] Muhanna, R.L., Zhang, H. and Mullen, R.L. (2007). “Combined axial and bending stiffness in interval finite-element methods.” *Journal of Structural Engineering*, 133(12), 1700–1709.
- [67] Mukhopadhyay, T., Chowdhury, R. and Chakrabarti, A. (2016). “Structural damage identification: a random sampling-high dimensional model representation approach.” *Advances in Structural Engineering*, 19(6), 908–927.
- [68] Murangira, A. Zuniga, M.M. and Perdrizet, T. (2015). “Structural reliability assessment through meta model based importance sampling with dimension reduction.” *hal-012304*.
- [69] Muscolino, G. and Sofi, A. (2017). “Analysis of structures with random axial stiffness described by imprecise probability density functions.” *Computers and Structures*, 184, 1–13.
- [70] Naveen, B.O. and Balu, A.S. (2017). “HDMR-based model update in structural damage identification.” *International Journal of Computational Methods*, 16(5), 1840004.
- [71] Rabitz, H., Alis, O.F., Shorter, J. and Shim, K. (1999). “Efficient input-output model representations.” *Computer Physics Communications*, 117, 11–20.
- [72] Rao, B.K. and Balu, A.S. (2019). “Modeling of delamination in fiber-reinforced composite using high-dimensional model representation-based cohesive zone model.” *Journal of the Brazilian Society of Mechanical Sciences and Engineering*, 41(6), 254.

- [73] Rao, B.N. and Chowdhury, R. (2009). “Enhanced high-dimensional model representation for reliability analysis.” *International Journal for Numerical Methods in Engineering*, 77(5), 719–750.
- [74] Schanz, R.W. and Salhotra, A. (1992). “Evaluation of the Rackwitz-Fiessler Uncertainty Analysis Method for environmental fate and transport models.” *Water Resources Research*, 28(4), 1071–1079.
- [75] Schöbi, R. and Sudret, B. (2017). “Structural reliability analysis for p-boxes using multi-level meta-models.” *Probabilistic Engineering Mechanics*, 48, 27–38.
- [76] Schöbi, R. and Sudret, B. (2019). “Global sensitivity analysis in the context of imprecise probabilities (p-boxes) using sparse polynomial chaos expansions.” *Reliability Engineering and System Safety*, 187, 129–141.
- [77] Simon, C. and Bicking, F. (2017). “Hybrid computation of uncertainty in reliability analysis with p-box and evidential networks.” *Reliability Engineering and System Safety*, 167, 629–638.
- [78] Sundar, V.S. and Manohar, C.S. (2014). “Estimation of time variant reliability of randomly parametered non-linear vibrating systems.” *Structural Safety*, 47, 59–66.
- [79] Sundgren, D., Danielson, M. and Ekenberg, L. (2009). “Warp effects on calculating interval probabilities.” *International Journal of Approximate Reasoning*, 50(9), 1360–1368.
- [80] Tunga, M.A. (2011). “An approximation method to model multivariate interpolation problems: Indexing HDMR.” *Mathematical and Computer Modelling*, 53(9–10), 1970–1982.
- [81] Ulaganathan, S., Couckuyt, I., Dhaene, T., Degroote, J. and Laermans, E. (2016). “High dimensional Kriging meta modelling utilising gradient information.” *Applied Mathematical Modelling*, 40(9–10), 5256–5270.
- [82] Valkó, V.T., Tomlin, A.S. and Turányi, T. (2017). “Investigation of the effect of correlated uncertain rate parameters on a model of hydrogen combustion using a generalized HDMR method.” *Proceedings of the Combustion Institute*, 36(1), 681–689.

- [83] Wang, C., Zhang, H. and Beer, M. (2018). “Computing tight bounds of structural reliability under imprecise probabilistic information.” *Computers and Structures*, 208, 92–104.
- [84] Wang, L., Wang, X. and Xia, Y. (2014). “Hybrid reliability analysis of structures with multi-source uncertainties.” *Acta Mechanica*, 225(2), 413–430.
- [85] Wang, X.J. and Qiu, Z.P. (2009). “Non-probabilistic interval reliability analysis of wing flutter.” *AIAA Journal*, 47(3), 743–748.
- [86] Wang, Z. and Chen, W. (2016). “Time-variant reliability assessment through equivalent stochastic process transformation.” *Reliability Engineering and System Safety*, 152, 166–175.
- [87] Wang, Z. and Wang, P. (2013). “A new approach for reliability analysis with time-variant performance characteristics.” *Reliability Engineering and System Safety*, 115, 70–81.
- [88] Wei, P., Song, J., Bi, S., Broggi, M., Beer, M., Lu, Z. and Yue, Z. (2019). “Non-intrusive stochastic analysis with parameterized imprecise probability models: II. Reliability and rare events analysis.” *Mechanical Systems and Signal Processing*, 126, 227–247.
- [89] Wei, P., Song, J., Lu, Z. and Yue, Z. (2016). “Time-dependent reliability sensitivity analysis of motion mechanisms.” *Reliability Engineering and System Safety*, 149, 107–120.
- [90] Wu, J., Luo, Z., Li, H. and Zhang, N. (2017). “A new hybrid uncertainty optimization method for structures using orthogonal series expansion.” *Applied Mathematical Modelling*, 45, 474–490.
- [91] Wu, Y.T. (1987). “Demonstration of a new, fast probability integration method for reliability analysis.” *Journal of engineering for industry*, 109(1), 24–28.
- [92] Xiao, N., Muhanna, R. and Mullen, R. (2016). “Static analysis of structural systems with uncertain parameters using probability-box.” In *International workshop on Reliable Engineering Computing (REC2016)*, Bochum, Germany.
- [93] Xiao, N., Mullen, R.L. and Muhanna, R.L. (2018). “Solution of uncertain linear systems of equations with probability-box parameters.” *International Journal of Reliability and Safety*, 12(1–2), 147–165.

- [94] Xiong, H., Chen, Z., Qiu, H., Hao, H. and Xu, H. (2012). “Adaptive SVR-HDMR meta modeling technique for high dimensional problems.” In *International Conference on Modeling, Identification and Control*, AASRI Procedia, Vol. 3, pp. 95–100.
- [95] Xie, S., Pan, B. and Du, X. (2017). “High dimensional model representation for hybrid reliability analysis with dependent interval variables constrained within ellipsoids.” *Structural and Multidisciplinary Optimization*, 56(6), 1493–1505.
- [96] Xu, J. and Kong, F. (2018). “A cubature collocation based sparse polynomial chaos expansion for efficient structural reliability analysis.” *Structural Safety*, 74, 24–31.
- [97] Yang, X., Liu, Y. and Ma, P. (2017). “Structural reliability analysis under evidence theory using the active learning kriging model.” *Engineering Optimization*, 49(11), 1922–1938.
- [98] Yang, X., Liu, Y., Zhang, Y. and Yue, Z. (2015). “Hybrid reliability analysis with both random and probability-box variables.” *Acta Mechanica*, 226(5), 1341–1357.
- [99] Yao, T.H.J. and Wen, Y.K. (1996). “Response surface method for time-variant reliability analysis.” *Journal of Structural Engineering*, 122(2), 193–201.
- [100] Zhang, H., Dai, H., Beer, M. and Wang, W. (2013). “Structural reliability analysis on the basis of small samples : An interval quasi-Monte Carlo method.” *Mechanical Systems and Signal Processing*, 37(1–2), 137–151.
- [101] Zhang, H., Mullen, R.L. and Muhanna, R.L. (2010). “Interval Monte Carlo methods for structural reliability.” *Structural Safety*, 32(3), 183–190.
- [102] Zhang, L., Zhang, J., You, L. and Zhou, S. (2019). “Reliability analysis of structures based on a probability-uncertainty hybrid model.” *Quality and Reliability Engineering International*, 35(1), 263–279.
- [103] Zhang, Q., Zeng, Z., Zio, E. and Kang, R. (2017). “Probability box as a tool to model and control the effect of epistemic uncertainty in multiple dependent competing failure processes.” *Applied Soft Computing*, 56, 570–579.
- [104] Zhang, X., Gao, H., Li, Y. and Huang, H. (2018). “A novel reliability analysis method for turbine discs with the mixture of fuzzy and probability-box variables.” *International Journal of Turbo and Jet Engines*.

- [105] Zhao, Y.G., Lu, Z.H. and Zhong, W. (2014). “Time-variant reliability analysis considering parameter uncertainties.” *Structure and Infrastructure Engineering*, 10(10), 1276–1284.
- [106] Zhu, B. and Frangopol, D.M. (2013). “Reliability assessment of ship structures using bayesian updating.” *Engineering Structures*, 56, 1836–1847.
- [107] Ziehn, T. and Tomlin, A.S. (2009). “Environmental Modelling & Software GUI–HDMR–A software tool for global sensitivity analysis of complex models.” *Environmental Modelling and Software*, 24(7), 775–785.

## **PUBLICATIONS**

### **JOURNALS**

1. Spoorthi, S.K. and Balu, A.S. (2019). “Failure probability of structural systems in the presence of imprecise uncertainties.” *Journal of The Institution of Engineers (India): Series A*. 100(4), 649–657. DOI: 10.1007/s40030-019-00393-9.
2. Spoorthi, S.K. and Balu, A.S. (2021). “Failure probability evaluation for systems with hybrid uncertainties.” *Engineering Structures*. (Elsevier Publishers, SCI indexed) (Submitted in January 2021; Under review).

### **CONFERENCES**

1. Spoorthi, S.K. and Balu, A.S. (2017). “Failure probability bounds using high dimensional model representation with p-box uncertain variables.” *International Conference on Structural Engineering and Construction Management*, Kandy, Sri Lanka, December 7–9.
2. Spoorthi, S.K. and Balu, A.S. (2017). “Response surface method for structural analysis with p-box uncertain variables.” *International Conference on Composite Materials and Structures*, IIT Hyderabad, India, December 27–29.
3. Spoorthi, S.K. and Balu, A.S. (2017). “Response surface method for structural analysis with imprecise uncertainties.” *International Conference on Theoretical Applied Computational and Experimental Mechanics*, IIT Kharagpur, India, December 28–30.
4. Spoorthi, S.K. and Balu, A.S. (2018). “HDMR based interval analysis for structural systems.” *National Conference on Multidisciplinary Design, Analysis, and Optimization*, IISc Bengaluru, India, March 23–24.
5. Spoorthi, S.K. and Balu, A.S. (2018). “Imprecise uncertainty analysis for structural systems.” *Structural Engineering Convention*, Kolkata, India, December 19–21.

## CURRICULUM VITAE

1. NAME : SPOORTHI S K
  2. DATE OF BIRTH : July 1, 1990
  3. EDUCATIONAL QUALIFICATIONS
    - Degree : Bachelor of Engineering (B.E.)
    - Specialization : Civil Engineering
    - Institute : Sri Taralabalu Jagadguru Institute of Technology,  
Ranebennur,  
Visvesvaraya Technological University, Belgaum  
Karnataka, India
    - Year : 2012
    - Degree : Master of Engineering Technology (M.Tech.)
    - Specialization : Structural Engineering
    - Institute : Government Engineering College, Haveri, Karnataka,  
India.
    - Year : 2014
    - Degree : Doctor of Philosophy (Ph.D)
    - Specialization : Structural Engineering
    - Institute : National Institute of Technology Karnataka, Surathkal,  
India
    - Registration Date : July 20, 2015
  4. ADDRESS : D/o ShankarRao Kulkarni  
"SPOORTHI", #17, 1<sup>st</sup> Main, 2<sup>nd</sup> Cross, Vikas Nagar,  
Ranebennur - 581 115, Karnataka, India  
Mobile: +91 9731753337  
Email: spoorthikulkarni@gmail.com
-